Marine Geology 289 (2011) 100–116

Contents lists available at SciVerse ScienceDirect

Marine Geology

journal homepage: www.elsevier.com/locate/margeo

Morphology and controls on the evolution of a mixed carbonate–siliciclastic submarine canyon system, Great Barrier Reef margin, north-eastern Australia

Ángel Puga-Bernabéu [a,b,*], Jody M. Webster [a], Robin J. Beaman [c], Vincent Guilbaud [d]

[a] Geocoastal Research Group, School of Geosciences, University of Sydney, Australia
[b] Departamento de Estratigrafía y Paleontología, Universidad de Granada, Spain
[c] School of Earth and Environmental Sciences, James Cook University, Australia
[d] Institut français de recherche pour l'exploitation de la mer (IFREMER), Brest, France

ARTICLE INFO

Article history:
Received 27 January 2011
Received in revised form 26 September 2011
Accepted 26 September 2011
Available online 1 October 2011

Communicated by D.J.W. Piper

Keywords:
submarine canyons
shelf-break
landslides
sandwaves
sediment gravity flows
sediment transport

ABSTRACT

We present the most complete and new high-resolution multibeam bathymetry datasets from the shelf to the basin in the Ribbon Reef region, northern Great Barrier Reef (GBR). Analysis of these data, combined with existing side-scan sonar data provides a detailed morphologic framework of the submarine canyon system and other related features, their spatial distribution, controlling factors on their evolution, and evidence of recent sedimentary activity. Two morphologically different submarine canyon types are recognised: 1) shelf-incised canyons whose heads are indented into the shelf-break at shallow-water depths (about 60 to 80 m). These canyons can be single-fed or multi-fed depending on the number of tributaries that merge into the main canyon valley. According to the degree of connection with the shelf, these canyons can be reef-blocked, partly reef-blocked or shelf-connected; 2) slope-confined canyons, which are located at deeper waters in the slope and show a different canyon head morphology. Canyon formation and development of the different canyon types is explained according to a four-phase model. In the first phase, localised slope failures and/or sediment gravity flows may lead to the formation of an initial canyon by retrogressive headward or downslope erosion respectively. These processes continue during the second transitional phase, leading to upslope canyon progression. Finally, canyons breach the shelf-break during a mature stage that represents the more active phase in the canyon evolution. The development of an extensive shelf-edge barrier reef (Ribbon Reefs) represents a fourth phase that conditioned the sedimentary dynamics of the canyons. The location and morphology of this reef barrier determine the type and amount of sediment supply by controlling the connection of the canyon head with the shelf drainage system. Recent canyon activity is evidenced by the presence of erosive and depositional features that include submarine landslides, gullies and rills on the canyon walls and slopes, sandwaves migrating along the canyons floors, and sediment gravity flows deposited on the lower canyons and adjacent basin floor.

1. Introduction

Submarine canyons are major morphologic features sculpting continental margins worldwide (Shepard and Dill, 1966; Shepard, 1972) and constitute the main conduits for shelf-to-basin sediment transport, independently of the tectonic setting (Carlson and Karl, 1988; Alonso and Ercilla, 2003; Lastras et al., 2009; Mountjoy et al., 2009). The best known examples of modern submarine canyons and their ancient counterparts correspond to siliciclastic systems (Lewis and Barnes, 1999; Babonneau et al., 2002; Anderson et al., 2006; Shanmugam et al., 2009). Modern and ancient submarine canyons in carbonate systems are relatively scarce in the literature (Leach and Wallace, 2001; Exon et al., 2005; Ruiz-Ortiz et al., 2006; Mitchell et al., 2007), and even less is known about submarine canyons in mixed carbonate–siliciclastic settings (Braga et al., 2001; Francis et al., 2008; Puga-Bernabéu et al., 2008).

The north-eastern continental margin of Australia is the largest mixed carbonate–siliciclastic province in the world (Maxwell and Swinchatt, 1970; Davies et al., 1991). Similar to other continental margins, large amounts of sediment are delivered into the deep ocean by different shelf-to-basin transport processes. On this margin, the amount and timing of siliciclastic and/or carbonate sediment supply to the basin is controlled by sea-level and climatic changes according to a transgressive shedding model of margin sedimentation (Dunbar et al., 2000; Dunbar and Dickens, 2003a; Page et al., 2003; Francis et al., 2007). In contrast to the conventional reciprocal model (Posamentier and Vail, 1988), these authors found that maximum siliciclastic fluxes to the slope over the last 30 ka occurred towards the end of the last transgression (peak about 10–11 ka) as sea-level flooded the shelf. Additionally, enhanced precipitation and

* Corresponding author at: Departamento de Estratigrafía y Paleontología, Universidad de Granada, Spain. Tel.: +34 958 242721; fax: +34 958 248528.
E-mail address: angelpb@ugr.es (Á. Puga-Bernabéu).

0025-3227/$ – see front matter © 2011 Elsevier B.V. All rights reserved.
doi:10.1016/j.margeo.2011.09.013

erosion driven by changes in monsoon hydrologic cycle during the early Holocene (Nanson et al., 1991; Nott and Price, 1994, Goodbred and Kuehl, 2000) could also have contributed to the siliciclastic pulse occurring during the shelf flooding. However, the role of submarine canyons in the processes operating within this transgressive shedding model has never been studied. This is in part because of the lack of detailed information about the structure and morphology of the sediment pathways from the shelf-to-basin (i.e. submarine canyons).

In this study, we present the most complete and high-resolution bathymetric dataset, integrated with existing GLORIA side-scan sonar images (Hughes Clarke, 1994), to provide the first detailed picture of the submarine canyons adjacent to the extensive Ribbon Reefs, here called the Ribbon Reef Canyons (RRCs), on the northern Great Barrier Reef (GBR) margin. We quantitatively describe the key geomorphologic characteristics of the submarine canyons and other related features, and discuss the processes involved in their origin, evolution, the controlling factors, and sedimentary activity. Sediments from the GBR contain geochemical and paleontological signatures of past climatic and environmental conditions, and are funnelled through the canyons to form part of the sedimentary record in the RRC system. This study provides a morphologic framework for future detailed research, and contributes to understanding the role of canyons in trapping shelf sediments and transport into the adjacent deep basin.

2. Regional physiography and sedimentology

The north-eastern Australia margin is a passive continental margin extending between about 14°S and 20°S latitude and 145°E and 150°E longitude (Fig. 1). This area can be divided into three broad physiographic regions: 1) the continental shelf and Great Barrier Reef; 2) the Queensland and Townsville Troughs, including the slope and basin environments; and 3) the Queensland Plateau, an isolated carbonate reef platform (Davies et al., 1991, Heap and Harris, 2008).

The study area lies in the northern part of the margin adjacent to an extensive shelf-edge barrier system, called the Ribbon Reefs (Fig. 2). These reefs are elongate, up to 28 km long (Hopley et al., 2007), and are separated by narrow inter-reef passages. Here, the shelf is relatively narrow (<50 km), with the shelf-break located at

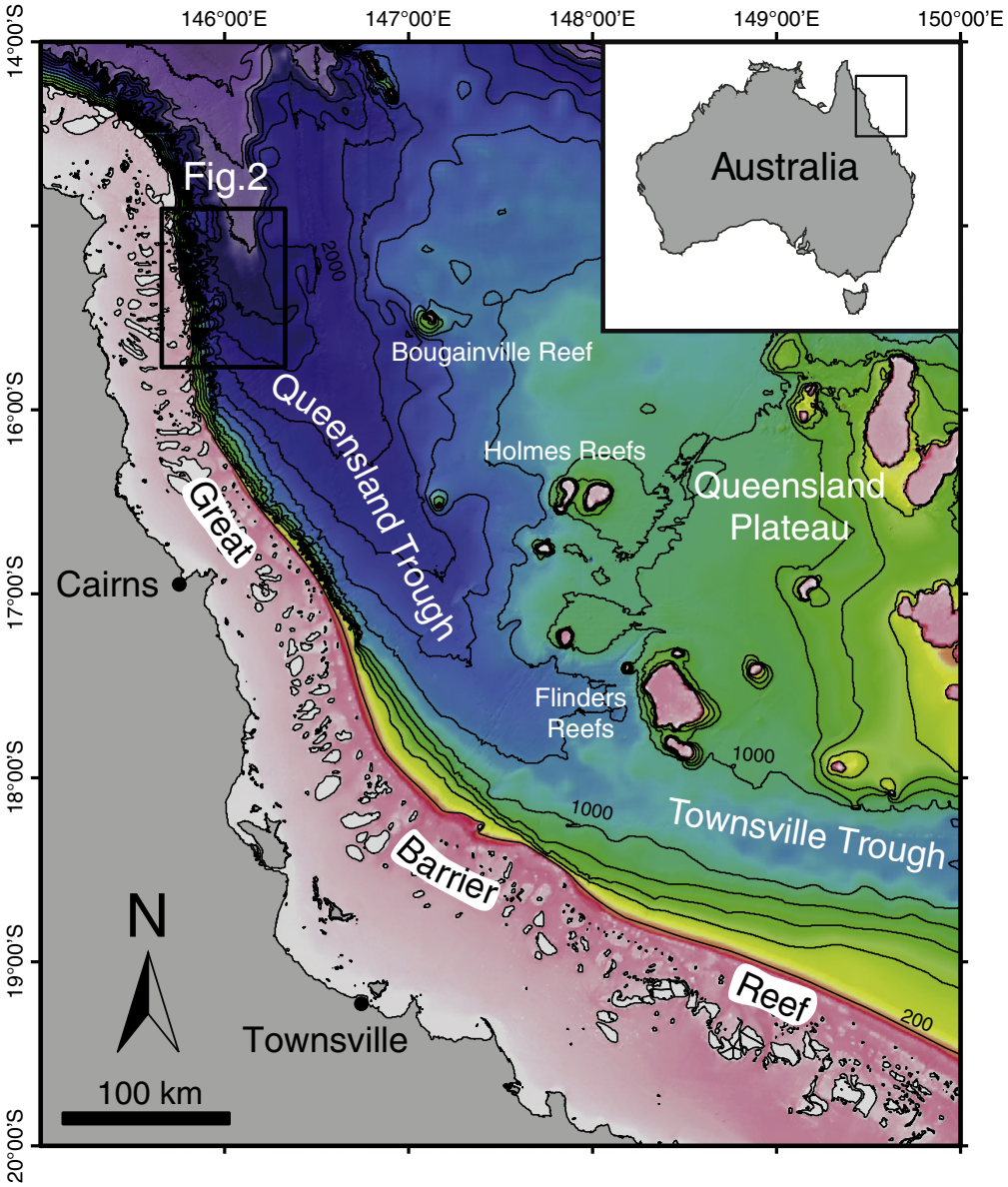

Fig. 1. General bathymetry (contours at 200 m intervals) of the northern Queensland margin showing the main physiographic regions: the Great Barrier Reef, Queensland and Townsville Troughs, and the Queensland Plateau. Inset shows the location of the study area in north-eastern Australia.

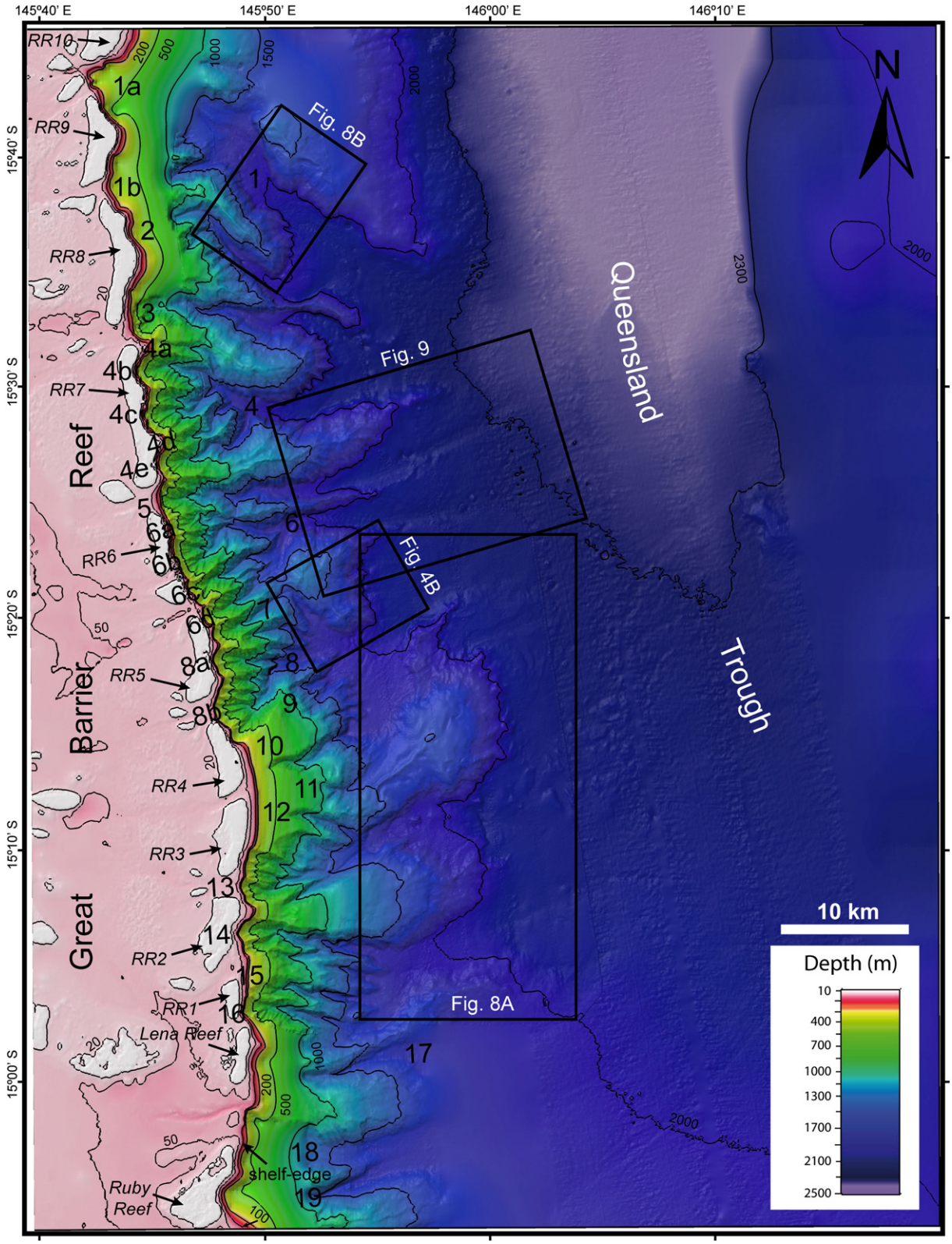

Fig. 2. Hillshaded map of the study area, from high-resolution multibeam data (RV *Southern Surveyor voyage* SS07/2007) and other data sources (see Beaman, 2010). Canyons are labelled with numbers (see Table 1 and text for canyon types). RR = Ribbon Reef. Additional key contour lines are given. Most of submarine canyons are shelf incised. Submarine canyons are essentially oriented perpendicular to the shelf-edge although abrupt changes of orientation are observed in Canyons 2 and 7. Note the intercanyon slope areas are overall narrow due to canyon proximity and that main non-excavated slope regions are located near the slope-confined and deep-water canyons. Also notice the presence of submarine channels in Canyons 5 and 6 that end in the Queensland Trough. Boxes refer to subsequent Figs. 4C, 8A, B and 9.

depths of 70 to 100 m, seaward of the Ribbon Reefs. The continental slope then drops steeply with numerous incised submarine canyons into the adjacent Queensland Trough. This trough is a narrow structural depression formed as a result of extensional tectonics during the Late Cretaceous and Tertiary (Symonds et al., 1983). In the study area, the Queensland Trough has a relatively smooth seabed

that gently deepens (average gradient <0.2°) to the north from about 2000 to 2500 m along the trough axis.

Modern sediments on the shelf comprise terrigenous siliciclastics and bioclastic carbonates (Maxwell, 1968; Francis et al., 2007). Carbonate content progressively increases offshore from about 20% on the inner-shelf, to about 60% on the middle-shelf, then to >80% on the outer-shelf. Within the Queensland Trough, recent sediments are similar in composition to those on the shelf: terrigenous siliciclastics (clays, feldspars and quartz) and biogenic carbonates of different mineralogies (aragonite, calcite and high-magnesium calcite; Dunbar and Dickens, 2003a, Francis et al., 2007). Sediment cores available from the study area reveal the presence of sediment gravity flow deposits (turbidites *sensu lato*) comprised of a spectrum of carbonate- to siliciclastic-dominated turbidites (Blakeway, 1991; Ludman 2007; Webster et al., 2008c). Based on new sedimentologic, geochemical and C14-AMS age data from these cores, Webster et al. (2008c) established the source, timing and frequency of turbidite events deposited in the canyons that occurred from the Late Pleistocene to present.

3. Material and methods

3.1. Bathymetry

The high-resolution bathymetry data were collected during the RV *Southern Surveyor* voyage in September–October 2007 (SS07/2007) using a Simrad EM300 multibeam echosounder (30 kHz) (Webster et al., 2008a,b). The raw multibeam data were processed using Caris HIPS and SIPS software to correct for sound velocity variations within the water column and to remove noise, and for creating bathymetric grids at different resolutions. The data were integrated with all available bathymetry data (see Beaman, 2010 for methods and data sources) to produce a 100 m-resolution grid for the entire region, and a close-up view of the study area. For this study, a 40 m-resolution grid has been used for the deeper area encompassing the submarine canyons, and a 5 m-resolution grid developed for a narrow area covering the shallower shelf-break.

3.2. Acoustic backscatter

The backscatter data are from the GLORIA side-scan sonar imagery (6.5 kHz) previously collected by HMAS *Cook* in July 1989. Despite the influence of seafloor roughness (here accentuated by the presence of submarine canyons and other submarine features) on the acoustic signature, the GLORIA imagery show areas of different acoustic responses that are not considered artefacts (Hughes Clarke, 1994; Fig. 3A). Although with limitations, acoustic backscatter can be correlated with grain size of surficial seabed sediments (Goff et al., 2000; Collier and Brown, 2005). Well-defined areas with high backscatter are here interpreted as coarse-grained deposits (sand–gravel) while low backscatter corresponds to fine-grained sediments (Hughes Clarke, 1994). Based on previous interpretations of the GLORIA imagery, Dunbar et al. (2000) identified four large sediment gravity flows originated in the continental margin and extending over the Queensland Trough.

3.3. Data integration and canyon labelling

The bathymetry grids and GLORIA images were imported into ESRI ArcMap 9.3. These datasets, in combination with derived slope maps (Fig. 3B) and bathymetric profiles, were used to study the location and spatial extent of the slope canyons and other features, and to characterise their morphology. Digital elevation models (DEMs) were generated using Fledermaus V7.1.2 software. These DEMs, together with draped GLORIA images and slope maps, were used to study the detailed 3D structure, morphology and surficial sediment texture of the submarine canyons and other features.

The canyons identified within the study area have been numbered from north to south independently of the canyon type (Fig. 2). Large tributaries (here called sub-canyons) within canyons are named with a subscript (1a, 1b, etc.) also from north to south.

4. Results

4.1. Submarine canyons

Submarine canyons of varying morphology and size incise at different depths along the shelf-edge and slope of the RRC region (Table 1, Fig. 2). These canyons incise most of the margin leaving relatively small non-excavated slope and interfluve areas. Two main types of submarine canyon are defined based on their incision depth: shelf-incised canyons (Type 1), and slope-confined canyons (Type 2). Canyons can also be divided into three different vertical zones: 1) the upper canyon zone, which comprises the canyon head and is commonly the area with higher gradients; 2) the middle canyon zone where the canyon is deeply incised and the gradient becomes less steep. In the study area, this zone corresponds with the 1400 m contour line; and 3) the lower canyon and basin zone, which includes areas of low gradient where the canyon becomes unconfined and merges into the basin floor. The metric characteristics and main morphologic parameters of each canyon are provided in Table 1 and Supplementary Tables 1, 2 and 3 respectively. The morphologic parameters are summarised in Tables 2 and 3.

4.1.1. Type 1: shelf-incised submarine canyons

These submarine canyons have well-developed, semicircular canyon heads, commonly with amphitheatre rims incised at shallow-water depths (60 to 135 m, Table 1).

Type 1 canyons are divided into two sub-types according to the confluence between canyons: single-fed canyons (Type 1a) which comprise a single canyon head connected to a single canyon valley (Canyons 2, 3, 5, 7, 13 to 19; Figs. 2 and 4), and multi-fed canyons (Type 1b) which comprise several sub-canyons that merge together downslope into a single channel (Canyons 1, 4, 6 and 8; Figs. 2 and 5). Although individual sub-canyons or tributaries in these latter canyons are similar to canyon Type 1a, they generally show a more complex morphology due to their closeness and the interaction of the sedimentary processes between tributaries.

One important aspect of this canyon type is the connection with the shelf, which is currently influenced by the presence of Ribbon Reefs along the shelf-edge. Different types of canyons, regardless of their morphology, can be recognised according to the shelf-to-canyon connections (Fig. 6):

1) Reef-blocked canyons. Open shelf supply to these canyons is significantly blocked by the presence of Ribbon Reefs (e.g. Canyons 2, 4, 7 and 19; Figs. 2 and 6). These reefs form a rim around the canyon heads and leave only a narrow shelf area seaward of the reefs. Shelf sediment supply to these canyons is therefore mainly restricted to reef-derived sediments.
2) Shelf-connected canyons. In these canyons, the heads have a wide and open connection with the shelf (e.g. Canyon 18; Fig. 6B) with only minor reef-blocking (e.g. Canyon 5; Fig. 6A).
3) Partly reef-blocked canyons. This includes canyons and sub-canyons whose heads are partly connected to the open shelf via inter-reef passages and also partly blocked by the Ribbon Reefs (e.g. Canyons 6 and 8; Figs. 2 and 6C). The degree of shelf connection is variable and ranges from mostly reef-blocked (e.g. Canyon 14; Fig. 2) to almost connected to the shelf (e.g. Canyon 13; Fig. 2).

Summarising, shelf-to-canyon connection seems independent of the canyon morphology. For example, large multi-fed canyons (Type 1b), such as Canyons 4 and 6, are morphologically similar

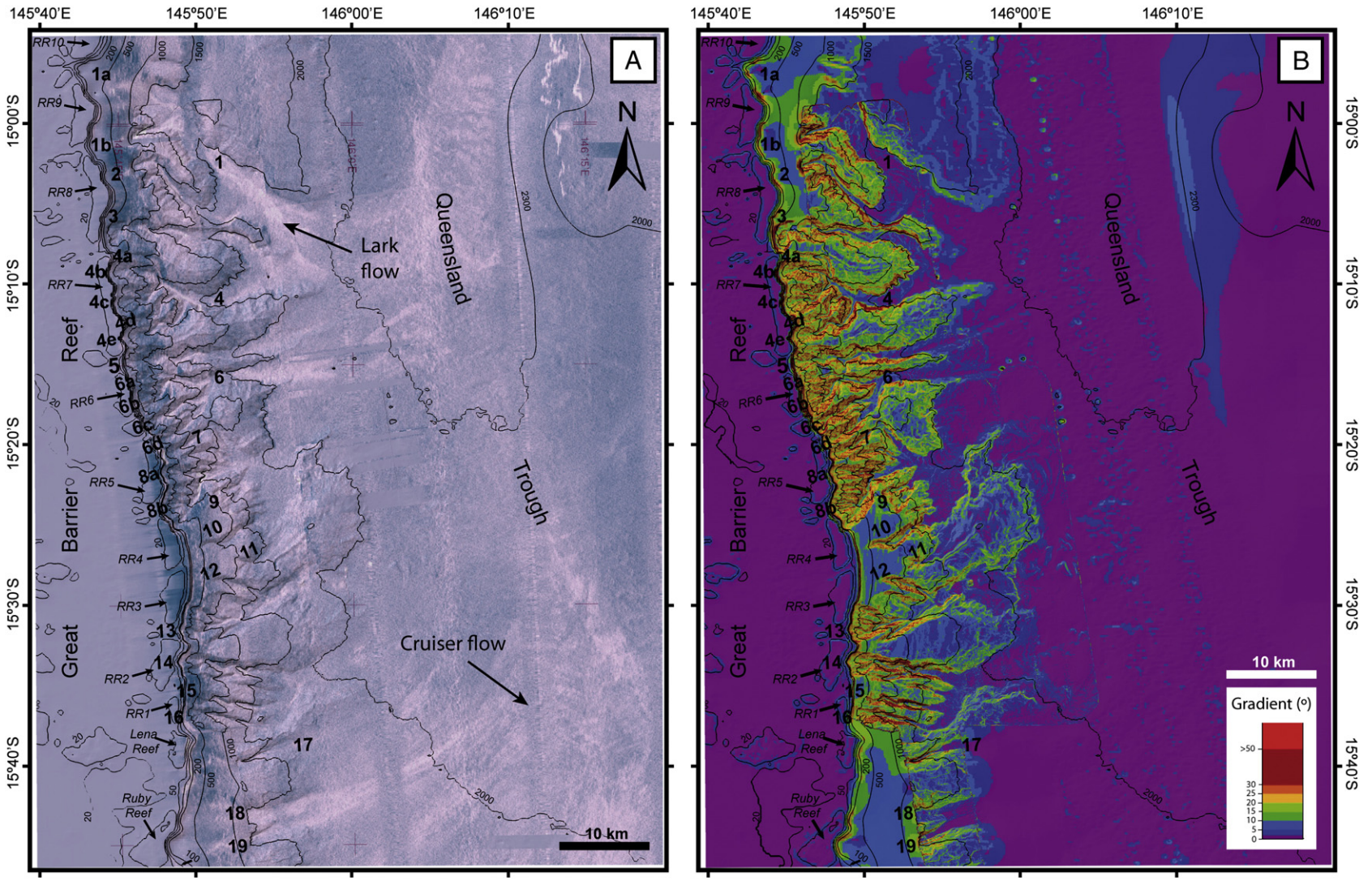

Fig. 3. (A) Hillshaded map of the study area with draped GLORIA side-scan sonar imagery from HMAS *Cook* (July 1989). Submarine canyons are marked with numbers (see Table 1 and text for canyon types). Note the presence of high backscatter (white-coloured) areas in the canyon valleys and towards the main axis of the basin. (B) Shaded slope map of the study area. Note the significant gradient changes at some canyon mouths.

Table 1
Summary of the metric characteristics of submarine canyons in the Ribbon Reef region.

C	Longitude (E)	Latitude (S)	Total length (m)	Straight length (m)	S	Max. width (m)	Av. width (m)	Max. floor width (m)	Max. In. (m)	Min. depth (m)	Max. depth (m)	Av. Gr.	Av. Slp.N	Av. Slp. S	Max. Slp. N	Max. Slp. S	G	Az.
1a	145°42′4.12″	14°56′7.95″	9164	8736	1.05	7880	7262	2200	533.1	76	2110	1.4	10.7	14.1	21.2	20.9	13	124
1b	145°42′47.93″	15°1′16.49″	–	–	–	–	–	–	–	58	1818	–	–	–	–	–	–	078
2	145°43′53.88″	15°3′19.28″	14598	11611	1.26	4830	3384	1110	618.2	66	2144	3.9	17.5	21.1	22.8	39.6	15	115
3	145°43′52.51″	15°7′38.52″	20461	17301	1.19	6010	4412	2500	739.3	68	2192	8.0	17.0	14.0	27.8	25.4	40	055
4	–	–	19349	16163	1.20	11480	8009	2035	815.3	34	2185	10.5	15.6	15.2	26.0	26.9	74	094
4a	145°45′3.36″	15°7′56.42″	20002	15478	1.29	1595	1117	126	246.7	346	1640	7.1	18.3	11.8	24.2	17.1	4	122
4b	145°44′4.82″	15°9′9.49″	19172	17360	1.10	3015	2442	185	618.2	45	1657	8.7	19.3	16.8	24.8	23.4	14	100
4c	145°44′23.10″	15°11′5.11″	18623	16665	1.12	4370	3049	300	615.9	34	1640	9.6	17.1	18.8	23.9	26.8	15	070
4d	145°45′31.45″	15°12′13.37″	18792	15222	1.23	1990	1422	500	713.7	282	1790	10.2	16.7	18.7	25.4	37.9	8	061
4e	145°45′0.97″	15°13′11.14″	20155	15993	1.26	3295	2483	525	603.9	140	1914	11.4	18.8	17.2	20.7	19.8	19	062
5	145°44′57.49″	15°14′48.97″	30049	28469	1.06	5920	3743	1050	720.1	61	2210	9.8	10.6	10.7	26.8	25.5	48	078
6	–	–	22376	20433	1.10	9470	5754	1245	611.2	60	2236	12.9	12.8	11.9	26.5	28.7	85	078
6a	145°45′30.42″	15°15′59.71″	22261	20240	1.10	1600	1297	100	326.9	78	1612	16.2	13.4	16.0	23.7	24.4	7	087
6b	145°45′55.28″	15°17′32.33″	22353	20704	1.08	3970	2892	1245	540.1	60	2236	14.2	18.4	18.8	26.7	25.3	36	065
6c	145°46′19.75″	15°18′29.83″	22326	20874	1.07	2495	1830	180	423.7	65	1766	11.8	20.7	19.5	28.4	35.1	22	058
6d	145°47′7.85″	15°19′56.33″	22561	19917	1.13	2490	1890	156	395.5	84	1883	13.6	17.6	18.8	26.2	28.7	20	043
7	145°47′30.66″	15°20′45.042″	12363	12072	1.02	3045	1927	662	352.9	65	1825	13.9	16.2	16.3	25.2	28.2	26	083
8	–	–	9958	9070	1.10	8070	4534	498	748.6	88	1876	11.1	20.2	18.4	30.2	22.4	48	056
8a	145°47′31.20″	15°21′45.22″	5674	5162	1.10	2450	1814	197	603.4	88	1576	17.9	22.4	19.8	30.2	31.0	16	094
8b	145°47′38.35″	15°24′10.67″	11508	10176	1.13	5910	3899	498	748.6	111	1876	9.8	20.9	18.8	43.5	22.4	26	056
9	145°50′53.10″	15°24′10.59″	7093	6304	1.13	3400	2470	628	380.4	821	1934	9.4	22.3	23.1	13.4	13.0	6	049
10	145°50′0.34″	15°26′20.87″	7511	6997	1.07	2050	1509	305	327.7	478	1822	12.1	18.0	17.7	24.2	27.6	6	067
11	145°52′27.72″	15°28′3.02″	6386	5975	1.07	3905	2258	595	422.6	1041	1683	5.9	10.6	7.4	19.0	14.0	4	053
12	145°50′51.79″	15°28′20.27″	6618	6437	1.03	2255	1527	150	347.2	666	1759	9.2	15.3	17.2	23.7	24.0	11	107
13	145°48′38.78″	15°31′24.70″	11371	10036	1.13	6490	4476	220	506.0	70	1768	10.9	13.4	18.1	21.9	23.2	26	073
14	145°48′31.14″	15°33′28.54″	13445	12704	1.06	3775	2317	1375	568.1	78	1902	8.9	20.8	21.8	33.0	36.4	34	099
15	145°48′57.55″	15°35′58.62″	11257	10737	1.05	2510	1556	1130	395.7	135	1791	13.2	18.5	18.4	35.4	27.0	27	093
16	145°48′44.11″	15°36′55.91″	12192	11410	1.07	2885	1905	1010	430.0	83	1766	11.4	18.2	16.5	32.0	28.0	39	093
17	145°49′6.96″	15°39′3.54″	6470	6364	1.02	3415	2949	906	463.8	73	1771	3.0	13.1	12.1	17.6	17.7	3	071
18	145°48′51.76″	15°41′8.16″	3163	3163	1.00	4380	3688	1220	570.3	84	1746	3.3	12.9	7.9	14.8	17.3	0	082
19	145°47′43.58″	15°44′47.53″	6001	5880	1.02	3860	3249	1215	681.6	70	1781	0.8	8.0	12.1	24.6	16.6	2	079

C = canyons; S = sinuosity; Max. = maximum; min = minimum; In. = incision; Av. Gr. = average gradient; Av. Slp. N = average slope of northern canyon flank; Av. Slp. S = average slope of southern canyon flank; G = number of gullies; Az. = azimuth (from head to mouth); regular font = shelf-incised canyons Type 1a; italics font = shelf-incised canyons Type 1b; bold font = slope-confined canyons Type 2.

despite Canyon 4 being fully reef-blocked and Canyon 6 having a variable degree of reef-blocking and shelf connection (Figs. 2 and 5). Even within the same partly reef-blocked canyons, the gully network and tributaries are similar regardless of whether they are reef-blocked or shelf-connected (e.g. Canyon 8; Fig. 6C).

4.1.2. Type 2: slope-confined canyons

Slope-confined canyons are canyons that do not breach the shelf-break (Canyons 9 to 12; Table 1, Figs. 2 and 7). Morphologically, two sub-types of canyons are defined: Type 2a and Type 2b. Type 2a canyons (Canyons 10 and 12) lack well-developed canyon heads and consist of small, narrow, triangular valleys excavated into the upper slope. Type 2b canyons (Canyons 9 and 11) have canyon heads located in deeper water depths of >750 m. The upper part of the canyon heads is poorly developed and resembles landslide surfaces (e.g. Canyon 9; Fig. 7) before grading downslope to an incised area with a gully network of differing degrees of incision.

In the middle canyon zone, these two canyons types show different cross-section profiles, and canyons walls are affected by small gullies and/or small landslides. In the lower canyon zone, knickpoints often occur near the canyon mouths, e.g. from 1520 to 1820 m over a distance of 1000 m in Canyon 10.

4.2. Intercanyon areas

The slope areas between the canyons are generally narrow and correspond to the interfluve edges of adjacent canyons (Figs. 2, 4A and 5A). Slope areas not excavated by canyons are mainly located in the southern half of the study area, between Canyons 8 and 14 (Figs. 2 and 7), and presumably between Canyons 17 and 19 (Fig. 2). This slope has average gradients between 7° to 10°, and is steeper (about 17°) in depths <250 m (e.g. Fig. 7C, profile b–b′). In some locations, these slopes occur as resistant promontories in deep-water (generally >1400 m) that may have influenced changes in the canyon courses (e.g. Canyons 2 and 7; Fig. 2).

4.3. Shelf features

As a result of Pleistocene sea-level fluctuations well-developed drowned reefs and palaeochannel features are preserved on the outer shelf and the narrow shoulder to seaward of the Ribbon Reefs (Beaman et al., 2008; Webster et al., 2011; Abbey et al., 2011). The excavated palaeochannels are observed cross-cutting the shelf, reaching different positions on the outer shelf. Some shelf-channels reach the shelf-break via the inter-reef passages before terminating in the canyon heads (e.g. Canyon 18, Fig. 6B), while others appear to end before reaching the shelf-edge (Fig. 6C). We find that there is no clear relationship between inter-reef passages, shelf-channels, canyon heads and general morphologic canyon type (Fig. 6).

4.4. Other deep-water sedimentary features

4.4.1. Submarine landslides and slope failures

Submarine landslides or slope failures are defined as areas of disturbed seafloor caused by the downslope movement of a failed mass (see McAdoo et al., 2000). These authors describe mass movements as: 1) blocky or cohesive for those submarine landslides with

Table 2
Main morphologic characteristics of Ribbon Reef Canyons Type 1.

	Shelf-Upper canyon	Middle canyon	Lower canyon-Basin
Canyon head	Semicircular to amphitheatre-like. Partly to fully reef-blocked, connected to inter-reef passages.		
Channel	Straight. Sinuous (Type 1b).	Variable.	Generally straight. Transition from sinuous to straight downslope (mainly in Type 1b).
Cross-section profile	Wide U-shape with superimposed smaller V-shape incisions.	V-shape (Type 1a). U-shape (Type 1b). Some transition V- to U-shape downslope.	U-shape.
Width	Uniform. Some increasing downslope (Type 1a).	Relatively uniform or decreasing downslope. Increasing locally due to confluences with tributaries and landslides (e.g. Canyon 13).	Relatively uniform or slightly decreasing. Local widening near the canyon mouth (mainly in Type 1a).
Wall slope	Variable.	Variable.	Uniform to decreasing downslope and one margin steeper than the other.
Gradient	Highest.	Decreasing downslope.	Uniform and low.
Incision	Relatively uniform to slightly increasing downslope.	Uniform to increasing.	Maximum. Generally decreasing downslope.
Other features	Well-developed gully network. Evidences of upslope erosion (e.g. Canyon 9).	Mostly residual interfluves. Knickpoints. Wall gullies.	Narrow interfluves. Knickpoints. Landslides at canyon mouth and walls. Submarine channel. Sandwaves along canyon floors. Blocks on canyon floor. Wall gullies.

allochthonous rubble at the base of the eroded seafloor (Fig. 8A); or 2) disintegrative for those submarine landslides that show no evidence of slide mass deposits adjacent to the failed area (Fig. 8A), either if the mass lost cohesion during failure or if it has subsequently disintegrated and/or become buried. Based on surficial morphology, the slumps here (Fig. 8A) are considered as cohesive landslides with a curved slip surface whose downslope limit is not exceeded by the failed mass (McAdoo et al., 2000).

In the RRC region, submarine landslides are mostly located in deep-water settings, generally >500 m. These landslides occur on: 1) the canyon sidewalls; 2) intercanyon slopes; and 3) near the base of the slope.

1) Slope failures developed on the sidewalls are mainly disintegrative and have headscarps mostly aligned subparallel to the canyon axis (Fig. 8B). These landslides are relatively small with a semicircular shape, and failure areas ranging from 0.7 to 7 km^2, with headscarp heights of between 18 and 132 m. Some landslides on the canyon flanks have incipient gullies and/or rills excavated into their surfaces (Fig. 8B).

Table 3
Main morphologic characteristics of Ribbon Reef Canyons Type 2.

	Shelf-Upper canyon	Middle canyon	Lower canyon-Basin
Canyon head	Triangular (Type 2a). Variable (Type 2b).		
Channel	Straight.	Variable.	Generally straight (Type 2a). Transition from sinuous to straight downslope (Type 2b).
Cross-section profile	V-shape (Type 2a). Wide U-shape with superimposed smaller V-shape incisions (Type 2b).	V-shape (Type 2a). U-shape (Type 2b).	V-shape or transition V- to U-shape (Type 2a). U-shape (Type b).
Width	Some increasing downslope (Type 2a). Uniform (Type 2b).	Relatively uniform or decreasing downslope.	Relatively uniform or slightly decreasing.
Wall slope	Similar at both margins.	Variable.	Uniform to decreasing downslope and one margin steeper than the other.
Gradient	Highest.	Decreasing downslope.	Locally highest due to knickpoints or landslides (e.g. Canyons 9 and 10).
Incision	Increasing downslope.	Uniform to increasing.	Generally decreasing downslope.
Other features	Evidences of upslope erosion (e.g. Canyon 9).	Knickpoints (Type 2b).	Knickpoints. Blocks on canyon floor (Type 2b).

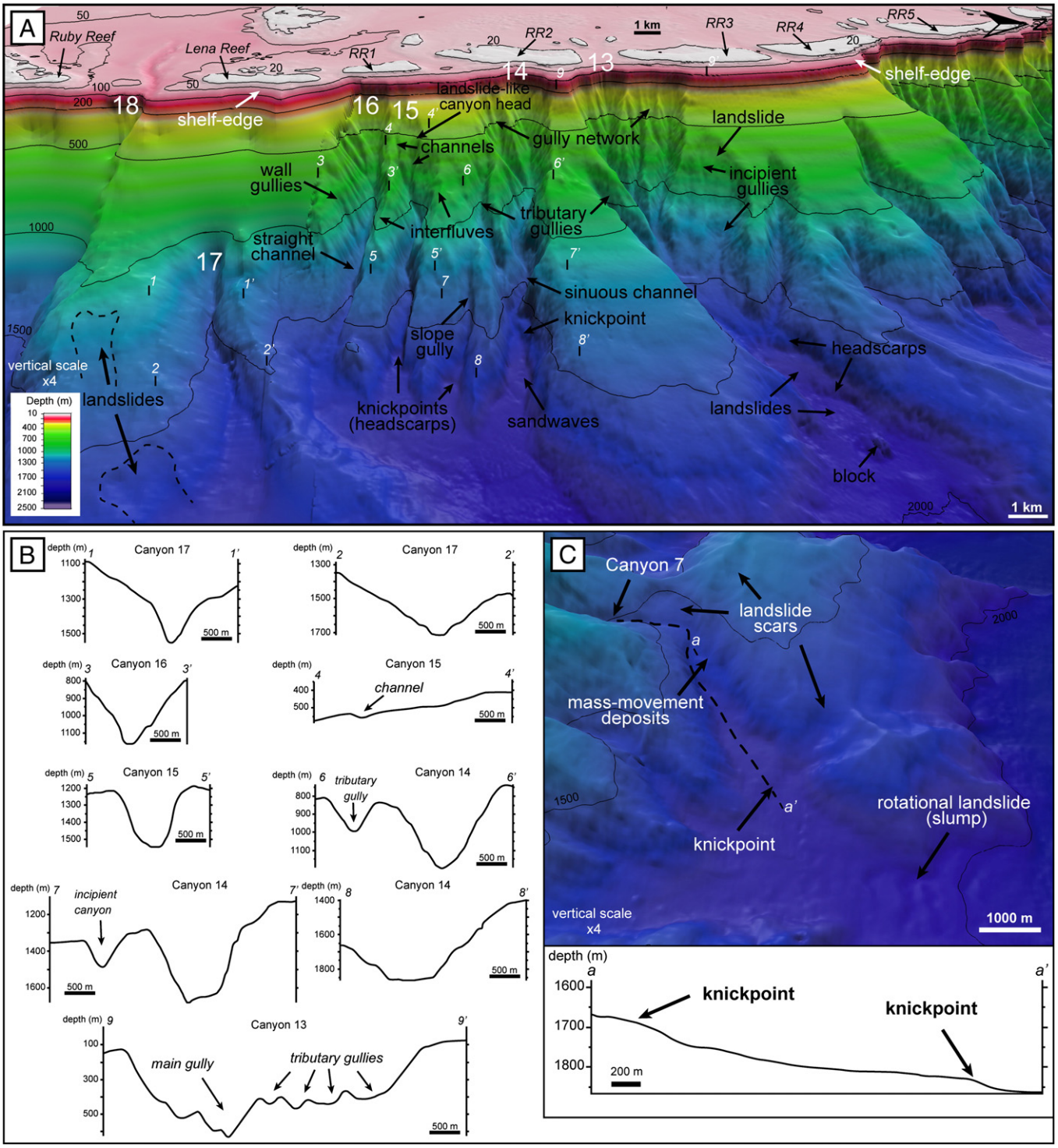

Fig. 4. (A) Digital elevation model (DEM) of representative examples of shelf-incised submarine canyons Type 1a (large white numbers) and adjacent areas in the Ribbon Reef region. Smaller numbers in italics indicate position of cross-section profiles shown in (B). Seabed features in the nearby areas are also marked. (B) Selected cross-section profiles from canyons in (A). (C) Close-up view from the lower part of Canyon 7 showing sidewall landslide scars and related mass-movement deposits that partly block the canyon floor. Depth profile below marks the position of knickpoints along the canyon axis. Note the abrupt change of direction of the canyon pathway (dashed line). Colour depth scale as in (A).

2) On intercanyon slopes, submarine landslides show elongated shapes and are comparatively larger in area than those on the canyon sidewalls. Headscarps are poorly developed, probably because their morphology is modified by the presence of gullies and rills, and/or these landslides may have evolved into large gullies and/or slope-confined canyons (e.g. Canyon 11; Fig. 7).

3) Landslides located at the base of the slope include cohesive, disintegrative and slump failures of variable shapes and sizes, from elongated to circular, failed areas up to 74 km^2 and headscarps up to 80 m in height. Some of these landslides are located at the canyon mouth or near the confluence of several canyons. Large knickpoints in the canyon floor near the canyon mouths, as found in Canyons 14 and 16 and adjacent gullies (Fig. 4), may be

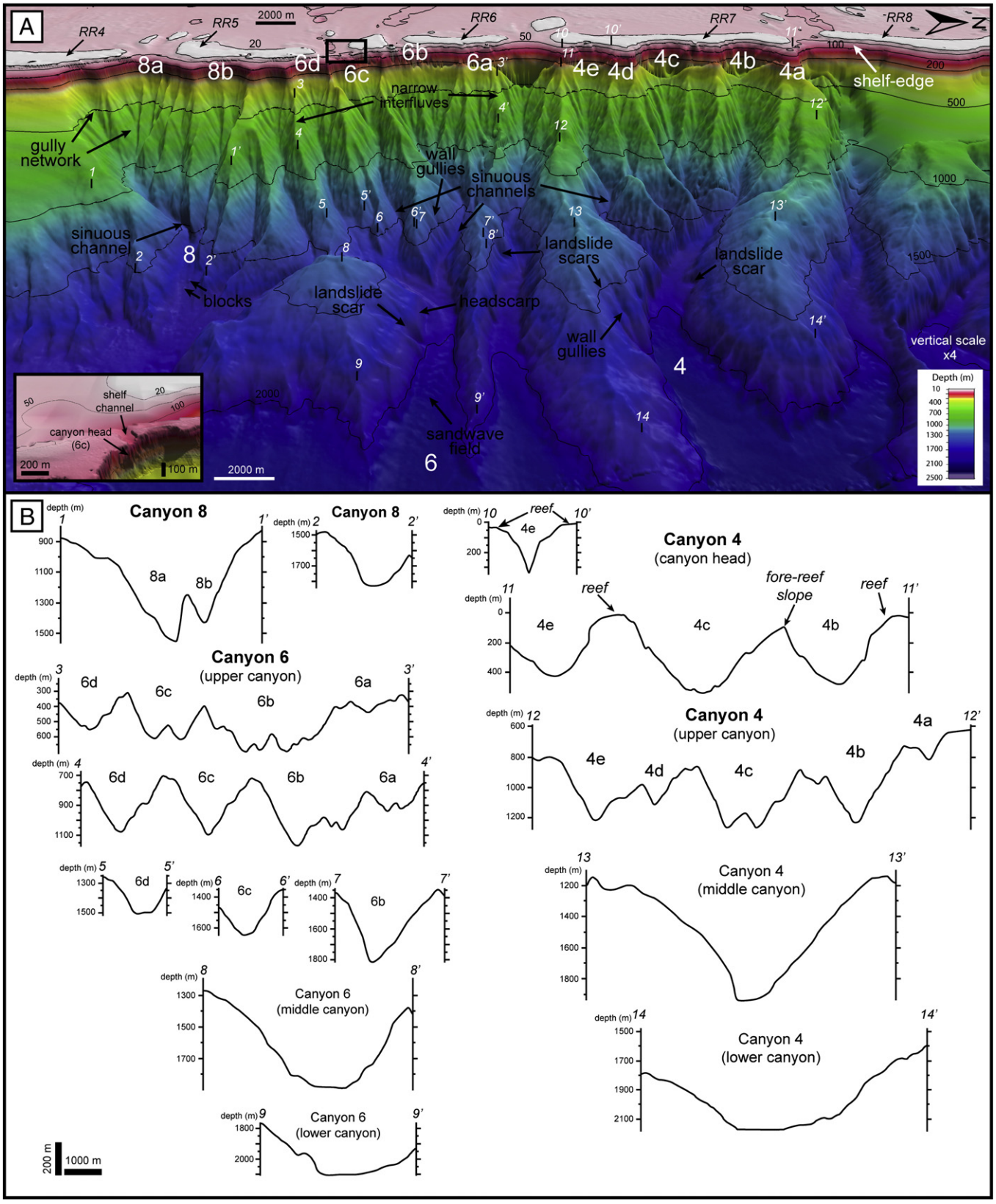

Fig. 5. Representative examples of shelf-incised submarine canyons Type 1b in the Ribbon Reef region. (A) DEM displaying canyon morphology and related features. Lower left corner inset shows high-resolution (5 m) view of a channel incised into the shelf-break and connected to Canyon 6c. Canyons are given in white. Numbers in italic indicate position of cross-section profiles shown in B). Note that Canyons 4 and 6 and are morphologically very similar regardless if they have different type of connection with the shelf (reef-blocked and partly reef-blocked). Canyons 4a and 4d are morphologically similar to slope-confined canyons. (B) Selected depth cross-section profiles from canyons in (A). Note down-canyon transitions from V- to U-shape cross-sections.

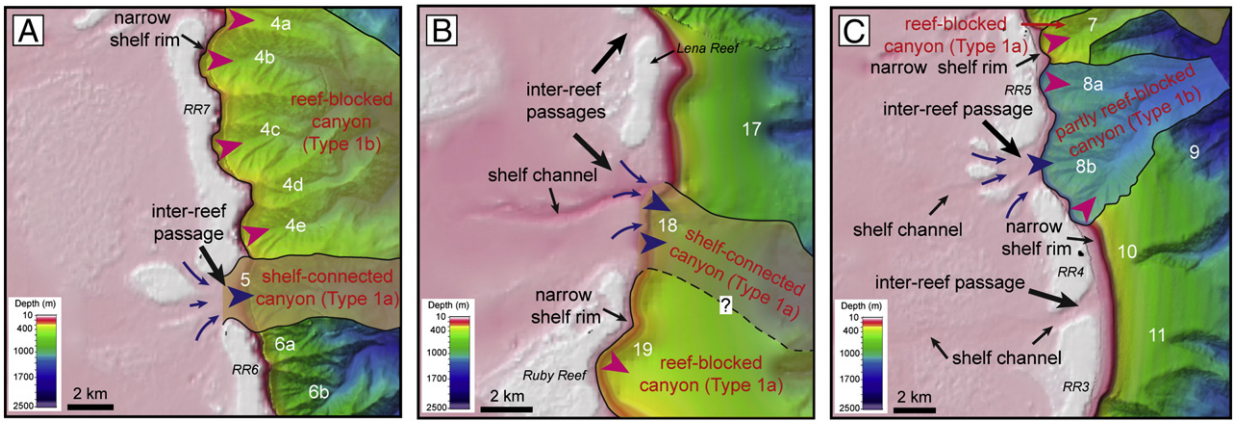

Fig. 6. Hillshaded maps of representative examples of shelf-incised submarine canyons according to their connection with the shelf. Arrow heads indicate the main source of sediment to the canyon heads, reef-derived (pink) or open shelf-derived (blue). (A) Large reef-blocked canyon (Canyon 4) and shelf-connected canyon (Canyon 5). Note that inter-reef passage linked to Canyon 5 is not related to any shelf-channel. (B) Reef-blocked canyon (Canyon 19) and shelf-connected canyon (Canyon 18). The latter canyon is connected to the shelf drainage system through a well-developed shelf-channel. (C) Partly reef-blocked canyon (Canyon 8) and small reef-blocked canyon (Canyon 7). Observe the presence of shelf-channels, some ending close to the shelf-edge and other several kilometres from it. These channels are not related to any specific canyon morphology.

the result of slope failure processes. Similarly, Canyon 9 resembles a larger submarine landslide (Figs. 2 and 7).

4.4.2. Submarine gullies and rills

In this study, rills are defined as small (<300 m wide and <60 m deep), straight channels developed in the canyon walls at different depths. Submarine gullies include larger, straight to sinuous channels developed in the canyons walls, at different positions across the slope and within slide scars (Figs. 4A, 5A, 7A and 8B). Gullies have a different scale compared to rills, from several 100 s of m to about 6 km long, and up to 2 km wide and 60 to 300 m deep.

Gullies that form part of the canyon heads are oriented nearly perpendicularly to the shelf-edge, forming a gully network where smaller tributary gullies and rills coalesce at different depths and extend into the main canyon channel. Gullies excavated at the canyon walls and base of the slope are generally oriented following the maximum gradient in the slopes. In contrast to the gullies found in canyon heads, the gullies in the canyon walls constitute single channels with only rare tributary confluences.

Large gullies are morphologically similar to slope-confined submarine canyons with rectilinear pathways (e.g. tributary gullies of Canyons 13 and 14, Figs. 5A and 7A). Some of these large gullies partially hang in the lower slope, with knickpoints and large gradient changes at the gully mouth.

4.4.3. Submarine channels

Most of submarine canyons in the study area are confined within wide U-shape canyon valleys at the base of the slope, where the gradient becomes less steep. Only Canyons 5 and 6 have thalwegs that continue as submarine channels across the basin after valley confinement (Figs. 2 and 9). Submarine channels are up to 200 m wide and up to 50 m deep, and follow a rectilinear pathway that becomes progressively shallower towards the basin. These channels have relatively short courses and end in the axis of the Queensland Trough. Sandwave fields (see Section 4.4.4) locally develop within these submarine channels (Fig. 9).

4.4.4. Sandwaves

A sandwave field extending over 5 km is observed along the thalweg of Canyon 6. This sandwave field starts in the middle canyon zone at about 2000 m near the confluence of tributary canyons and extends towards the lower canyon to depths of about 2130 m (Fig. 9). Sandwaves range in wavelength from 190 to 580 m (average 370 m), from 4 to 17 m in height (average 12 m), and are distributed along a downslope gradient of 1.5°. Although the grid resolution does not permit identifying all the sandwaves, they appear rectilinear-crested or barchan shape spanning the whole channel (Fig. 9). These sandwaves correspond to coarse-grained sediment waves using definitions according to Wynn and Stow (2002). Similar but smaller sandwave fields are also developed near the mouth of Canyon 14 (Fig. 4), although not fully resolved within the current grid resolution.

4.4.5. Sediment gravity flows

GLORIA side-scan images reveal the presence of sediment gravity flow (SGF) deposits on the seafloor along canyon valleys and in the basin (Figs. 3A and 10). These relatively coarse-grained deposits are characterised by high acoustic reflectance (white-coloured), occurring on top and/or between low reflectance, finer-grained, slope and basin hemipelagic/pelagic sediments (Hughes Clarke, 1994). In shelf-incised canyons (Type 1), these sediments accumulate in the middle canyon where the gully network passes downslope to the main channel. These deposits are especially abundant in Canyons 4 (a reef-blocked canyon) and 6 (a partly reef-blocked canyon) (Figs. 3A and 10).

Significant SGF deposits occur along canyon courses and extend into the basin over a few 10s of km from Canyons 1, 4, 6, 18 and 19, and to a lesser extent from Canyons 3 and 5 (Fig. 10). In these submarine canyons, individual SGF deposits are narrow and elongated in plan view, and may coalesce with similar deposits from adjacent canyons (Fig. 10). These larger flows correspond to the Lark and Cruiser flows identified by Dunbar et al. (2000) (Figs. 3A and 10). The largest flows reach the Queensland Trough and fill its axis. SGFs derived from Canyons 18 and 19 and other flows coming from the south of the study area do not follow a rectilinear pathway but are deflected to the north (Fig. 10). On the basin floor, there are also areas with high reflectance backscatter that may correspond to previous SGFs and/or mass-transport deposits but are now covered by younger hemipelagic/pelagic sediments (Fig. 10).

5. Discussion

5.1. Origin and evolution of submarine canyons

Two main hypotheses have been proposed to explain the origin and development of submarine canyons along continental margins and include: 1) river erosion and/or erosion under shallow-water conditions; and 2) slope failure and retrogressive (headward) erosion (Farre et al., 1983; Pratson and Coakley, 1996; Harris and Whiteway, 2011).

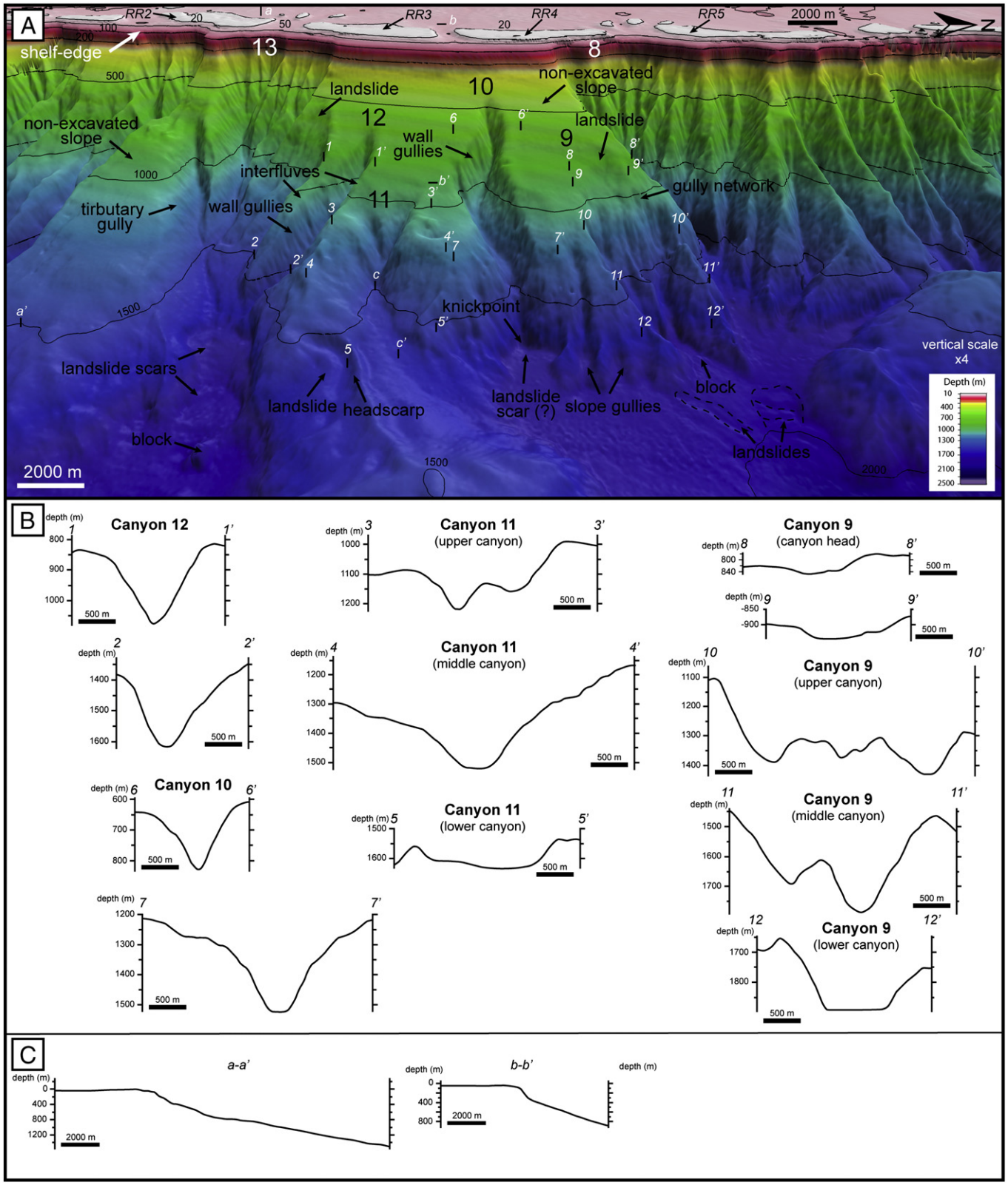

Fig. 7. (A) DEM of slope-confined canyons (large black numbers) (see Table 3 for canyon type) and adjacent areas in the Ribbon Reef region showing canyon morphology and related features. Numbers and letters in italic indicate position of profiles shown in (B) and (C) respectively. Canyons 9 and 11 resemble submarine landslides. Head of Canyon 11 corresponds to a slide surface. Observe the presence of landslide scars at some canyon mouths. (B) Selected depth cross-section profiles from canyons in (A). Note the low-relief morphology of the slide surface in the head of Canyon 11. (C) Depth profiles across the non-excavated slopes showing their morphology (a–a′ and b–b′) and depth profile through the axis of Canyon 11 (c–c′) with marked positions of knickpoints.

1) River erosion and erosion under shallow-water conditions can occur in the upper reaches of submarine canyons when relict fluvial courses are active during sea-level falls and sea-level lowstands (Babonneau et al., 2002; Antobreh and Krastel, 2006; Puga-Bernabéu et al., 2008). Downward processes in shallow marine settings, including hyperpycnal (near bottom) flows

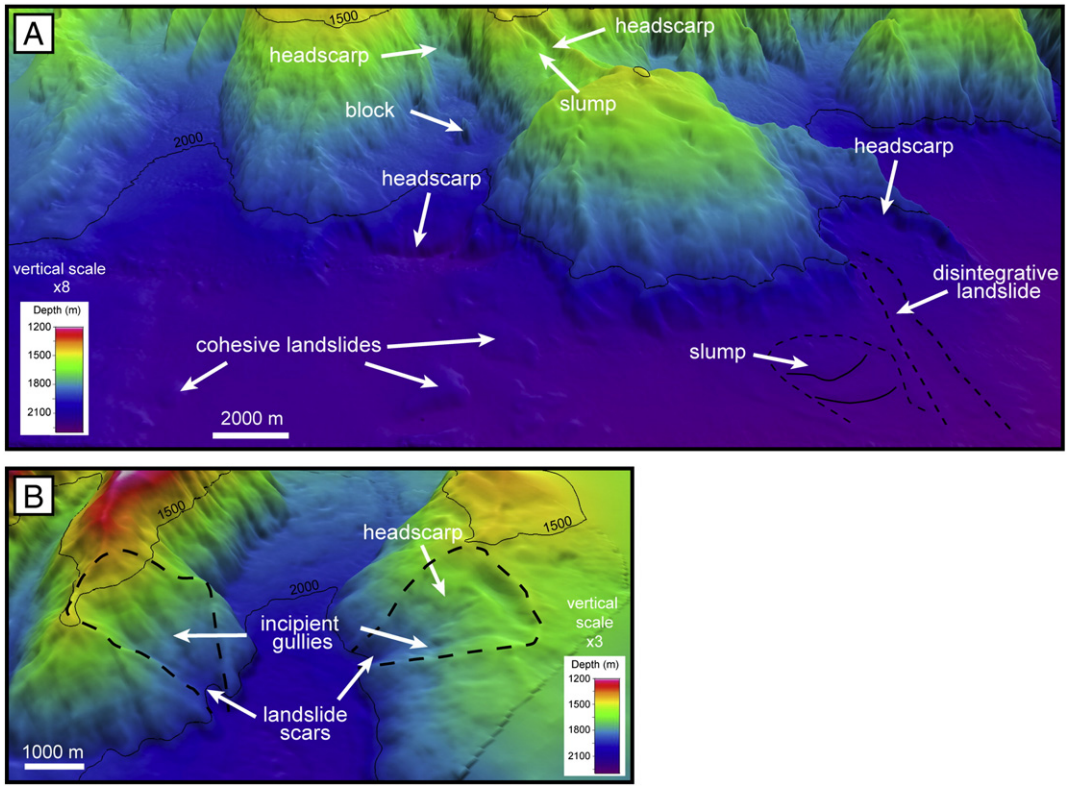

Fig. 8. (A) DEM from lower-slope areas (see Fig. 2 for location) showing different types of submarine landslides in the study area. (B) DEM from lower canyon reaches (see Fig. 2 for location) marking submarine landslides (black dashed lines) in the canyon walls.

(Mulder et al., 2003; Popescu et al., 2004; Baztan et al., 2005), storm- and current-driven erosive flows (Shepard et al., 1974; Inman et al., 1976; Puig et al., 2003), and other erosive flows (turbidity flows *sensu lato*) of different origin (Daly, 1936; Beer and Gorsline, 1971), lead to seaward excavation and entrenchment of submarine canyons across continental slope to the basin floor.

2) Slope failure and retrogressive erosion can occur on the continental slope at different depths, independently of sediment input and sea-level variation. Mass failure processes can be triggered by slope oversteepening (Pratson and Coakley, 1996; Hühnerbach et al., 2005), fluid and/or gas venting in the continental slope (Carpenter, 1981; Orange and Breen, 1992; Dugan and Fleming, 2000), tectonic deformation/faulting and earthquakes (Ridente et al., 2007; Green and Uken, 2008).

These mechanisms of canyon inception therefore condition the canyon morphology, although internal canyon variability and complexity (Soh and Tokuyama, 2002; Chiang and Yu, 2006) may obscure the relationship between canyon morphologies and their genesis. Thus, shelf-indenting canyons (here Type 1) are generally thought to be linked to river erosion and/or downward eroding sediment

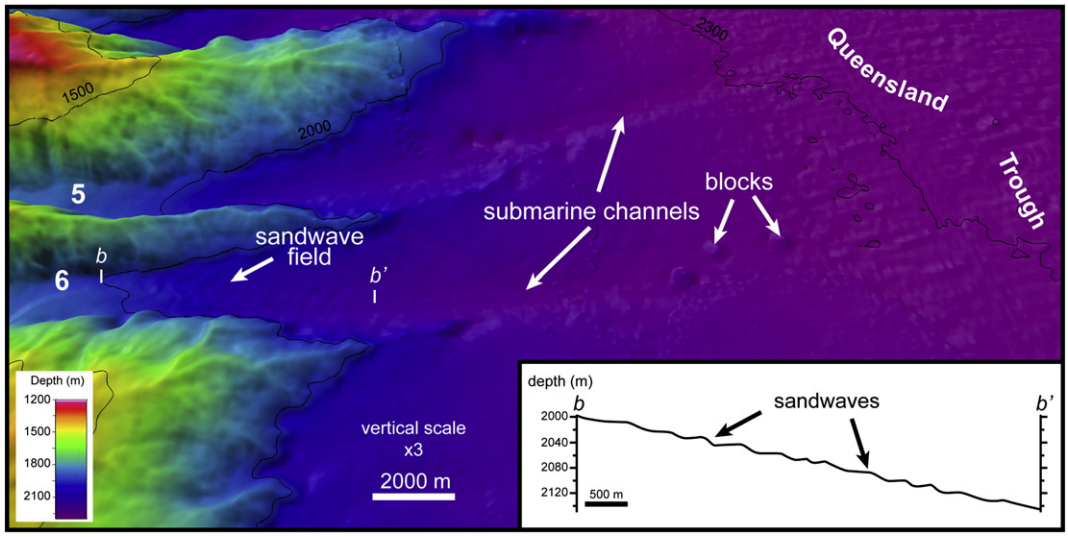

Fig. 9. DEM showing submarine channels continuing from Canyons 5 and 6 (white numbers) and selected depth profiles. Channels extend into the Queensland Trough. Observe the presence of a sandwave field in Canyon 6. Sandwaves have rectilinear crests and crescent shapes.

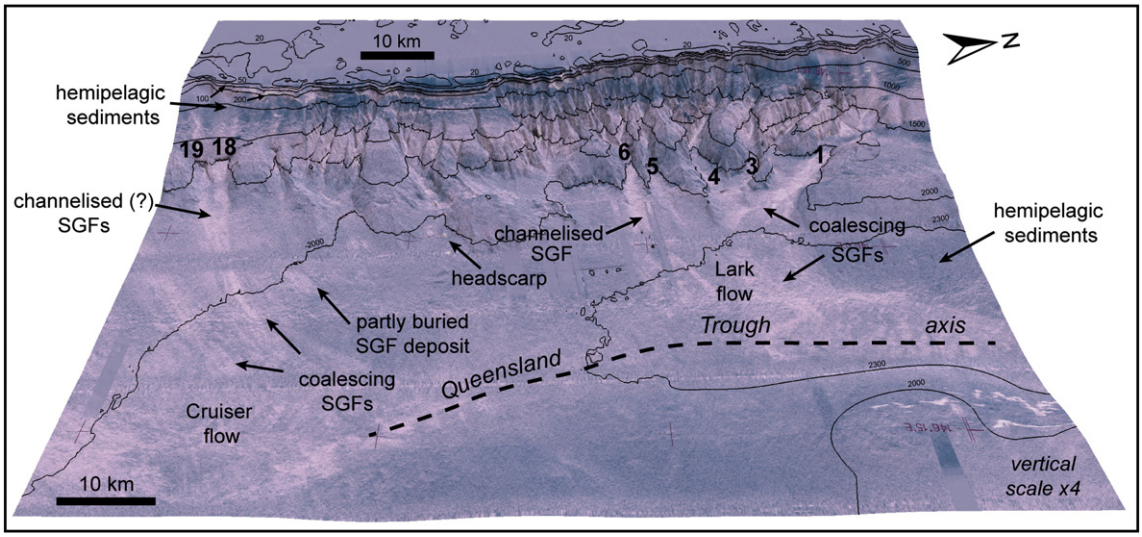

Fig. 10. DEM with draped backscatter imagery from Fig. 3. High-reflectivity (white-coloured) sediment gravity flow (SGF) deposits occur at the mouths of some submarine canyons (canyon numbers in bold) and extend into the axis of the Queensland Trough. Note that many of these flows, sourced from different canyons, merge together and form large SGF deposits known as Lark and Cruiser flows (Dunbar et al., 2000). Other significant seabed features are also marked.

gravity flows (Pratson et al., 1994; Kineke et al., 2000; Popescu et al., 2004; Baztan et al., 2005), while the onset of slope-confined canyons (here Type 2) is attributed to slope failure and upslope retrogressive erosion (Orange et al., 1997; Elliott et al., 2006; Green et al., 2007). However, the integrated model of canyon formation proposed by Twichell and Roberts (1982) and Farre et al. (1983), and modified by Pratson and Coakley (1996), reconcile the two main canyon morphologies and inception mechanisms.

Based on our analysis of the geomorphic data we suggest that the formation of RRC system generally follows the model of Farre et al. (1983). This model consists of three phases, where down- and upslope processes interact to shape the submarine canyons. In the Ribbon Reef region, we also argue that the extensive shelf-edge barrier reef influenced the sediment sources and pathways into the canyons since its formation 500 to 700 ky ago (Webster and Davies, 2003; Braithwaite and Montaggioni, 2009) and thus represents another important evolutionary stage.

Phase 1: initial or youthful stage. Pre-conditioning factors such as low sediment strength, differential compaction in the sediment, permeability, underconsolidation, or the presence of faults and other tectonic structures lead to localised slope failures (Fig. 11, phase 1a). Triggering factors could include fluid escapes, earthquakes and sediment overpressure by rapid deposition, and/or oversteepening.

In the study area, submarine landslides of different sizes occur in lower-slope regions with relatively low gradients (Figs. 4 and 8) and also in some canyon mouths (Figs. 4 and 6). These landslides represent the initial phase of canyon formation but their growth upslope will depend on the changing conditions (e.g. subsequent infilling with hemipelagic sediments, erosion along structural fabrics, and sediment consolidation; Farre et al., 1983). If conditions are favourable, upslope retreat of the failed surfaces by progressive sediment destabilisation and retrogressive erosion leads to the formation of an initial submarine canyon (Fig. 11, phase 1b). We observe this scenario in the study area with slope-confined canyons (Type 2) at the base of the slope (Fig. 7). Additionally, erosive sediment flows derived from failed material could excavate axial incisions in the landslide scars (e.g. Canyon 9, Fig. 7) that would contribute to the headward erosion of the canyon (Pratson and Coakley, 1996).

Pratson and Coakley (1996) point to the existence of precursor rills formed by downslope erosive flows triggered in the upper slope by sediment oversteepening, leads to the canyon-forming slope failures. There is no surficial evidence of these features in the upper slope of the study area. However, given the lack of subsurface data we cannot fully discount the presence of buried rills in the upper slope. Therefore, the formation of the initial submarine canyons by downslope eroding flows (Fig. 11, phase 1b) cannot be discarded.

Phase 2: transitional stage. In this phase the initial canyons progress upslope to near the shelf-break (Fig. 11, phase 2). Canyon growth mechanisms are similar to phase 1. Morphologic evidence for this stage is observed in Canyon 9 where the upper part shows incipient sediment sliding (Fig. 7). The presence of a partially failed area with incipient rills in the intercanyon area between Canyons 12 and 13 (Figs. 4 and 7) also supports a transitional stage. Similarly, Canyon 15 which is slightly incised in the shelf and whose canyon head resembles a slide scar with axial incised gullies (Fig. 4) represents a canyon in a transitional stage. In this canyon, downslope sediment gravity flows from the shelf likely contributed to canyon incision.

Phase 3: mature stage. This phase involves a change in the erosion style of the canyons which may breach the shelf-edge (Fig. 11, phase 3) due to progressive upslope erosion. This stage is represented by shelf-incised submarine canyons (Type 1). The canyon heads act as catchment areas for shelf and river sediments (Herzer and Lewis, 1979; Mullenbach et al., 2004; Green, 2009) that bypass the slope through the canyon valleys and are deposited on the basin floor. Submarine canyons become more active due to the increased sediment supply provided from different areas on the shelf. Downward sediment gravity flows can contribute significantly to ongoing canyon excavation and enlargement by axial incision and linked wall collapses (Pratson and Coakley, 1996; Popescu et al., 2004; Baztan et al., 2005). As a consequence, a network of downward connected gullies

Fig. 11. Model of canyon formation and development in the Ribbon Reef region based on morphological characteristics of the canyons. Sketches to the left and example DEM sections observed in the study areas on the right correspond to the different stages of canyon evolution. Geological weakness in the slope sediments may result in a slope failure in the initial stage (1a). Depending on the local conditions, the resulting landslide could evolve by retrogressive sediment destabilization into an incipient canyon (1b). Although not evidenced from multibeam bathymetry, downslope eroding sediment gravity flows may also induce initial canyons in the upper slope. Growth of young canyons by progressive headward erosion and related processes extend the canyon head nearer to the shelf-edge in the transitional stage (2). In the mature stage (3), submarine canyons breach the shelf-edge and receive sediment supply from the shelf that contributes considerably to canyon enlargement. The final reef-blocking stage (4) modifies the sedimentary dynamic of the canyons by determining the type and source of sediment to the canyon heads (i.e. reef-sourced and/or open shelf-sourced).

develops, forming an amphitheatre-like canyon head. Similarly at this stage, different canyon valleys may coalesce into a larger one, forming multi-fed, shelf-incised submarine canyons (Type 1b) (e.g. Canyons 4, 6 and 8, Fig. 5). Moreover, downslope and upslope processes can act together to maintain and enlarge these submarine canyons in their mature phase.

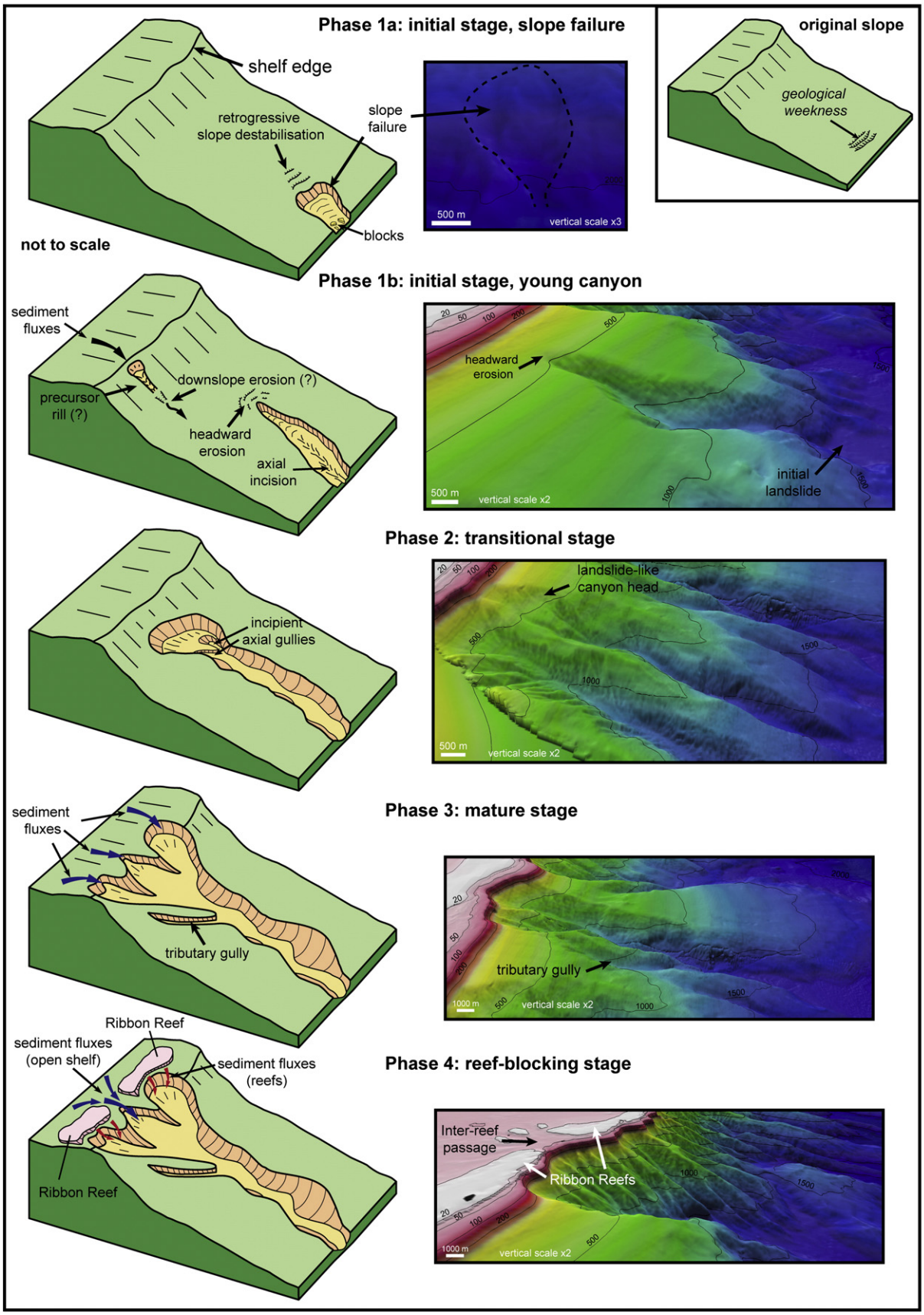

Phase 4: reef-blocking stage. Ribbon Reef formation likely changes the dynamics of sediment delivery into some canyons (Fig. 11, phase 4). Whether fully, partially, or unblocked by reefs (Fig. 6), the sediment supply into the canyons, and thus the type and frequency of eroding sediment gravity flows responsible of their excavation, is different (see Section 5.3). The morphology of the shelf-incised canyons that are fully blocked by reefs is similar to those canyons either partially blocked by reefs or open to the shelf (Figs. 2, 4, 5 and 6). This suggests that these canyons were excavated and developed their complex morphology before the development of the Ribbon Reef barrier influenced the sedimentary dynamics.

Our model is consistent with the observations and explains the presence of the different canyon morphologies, including the intermediate morphologies between the Type 1 and 2 canyons. While the influence of downslope eroding processes cannot be completely discarded, several lines of evidence suggest that upslope eroding processes dominate. First, the presence of shelf-channels that reach the outer shelf is not always related to the existence of shelf-incised canyons (Fig. 6C). Second, abrupt changes in gradient (landslide scarps) at the mouth of slope-confined canyons and canyons in a transitional stage (e.g. Canyons 10, 13 and 15; Figs. 4A and 7A) suggest an origin from initial failures at the base of the slope. Third, canyons in initial or transitional stages (e.g. Canyons 9 to 12; Fig. 7) occur in slope areas less excavated by canyons (i.e. south from Canyon 8; Fig. 2) while more mature canyons are in the same highly eroded slopes areas (Fig. 2). Fourth, if the entire RRC system was formed by downslope eroding processes, the number of canyons and the degree of slope erosion should be similar along the margin. Finally, while there is no evidence of buried canyons, we argue that their presence would not substantially modify our model as they would likely only act as preferential pathways for erosion.

5.2. Sedimentary dynamics in Ribbon Reef Canyons

We find abundant morphologic evidence of recent canyon activity that includes the presence of erosive and depositional features on the canyons and in the deeper basin, such as slope failures and related features (e.g. headscarps, cohesive and disintegrative landslides, and slumps), sandwaves, and SGF deposits.

The occurrence of sandwaves on submarine canyon thalwegs has been reported in modern canyons such as the Monterey Canyon (Smith et al., 2005, 2007; Xu et al., 2008) and the Setúbal Canyon (Arzola et al., 2008). In the Ribbon Reef Canyons, these sedimentary bedforms are not as abundant and well-developed but indicate similar sedimentary processes. Sandwaves in confined (canyon channel) deep-water environments result from the action of downslope sediment gravity flows, and/or upslope tidal currents, or internal waves through the canyon axis (Karl et al., 1986; Wynn and Stow, 2002; Shanmugam, 2003). Submarine sandwave morphology is influenced by various factors such as the grain size, water depth, current speed, spatial change in the canyon floor or slope gradient (Ashley, 1990; Bartholdy et al., 2005; Smith et al., 2007; Xu et al., 2008). High to moderate backscatter suggest that the sandwave field is characterised by relatively coarse-grain sized sediments (sand-gravel; Hughes Clarke, 1994). Further, rectilinear crests and barchan sandwave morphologies (Fig. 9) suggest a down-canyon migration (Wynn and Stow, 2002; Wynn et al., 2002; Xu et al., 2008) under current speeds of 50–80 cm/s (Wynn et al., 2002; Xu et al., 2008).

The main depositional process acting in the canyons is the deposition of SGFs. Sediments moving along the canyon floors are generally exported downslope for varying distances depending on the sediment type and flow characteristics (Mulder and Alexander, 2001). Most of the shelf-incised canyons contain well-developed SGF deposits, while they are absent in slope-confined and deep-water canyons (Fig. 10). In the study area, SGF deposits have been previously recognised as two large proximal gravity flows called Lark flow to the north, and Cruiser flow to the south (Figs. 3A and 10). Our new data show that the Lark and Cruiser flows are not single flows but rather formed by several SGFs sourced from different canyons, regardless of their morphology and shelf-connection type (e.g. Lark flow comprises of SGFs derived from canyon Types 1a and 1b, including reef-blocked, partly reef-blocked, and shelf-connected canyons; Fig. 10). These SGF deposits build sedimentary bodies that can be interpreted as small sediment lobes, which are similar in size to those linked to submarine canyons in the California Continental Borderland (Piper et al., 1999) and Corsica (Kenyon et al., 2002; Deptuck et al., 2008).

In contrast to pure siliciclastic or carbonate systems, we suggest that the complex configuration of the shelf-margin and adjacent canyons in the Ribbon Reef region strongly influences the sedimentology of the SGF deposits and the building of sediment lobes. SGF deposition through canyons with open connections to the shelf-edge and shelf-channel (e.g. Canyon 18, Fig. 6B) will be influenced by sea-level fluctuations that control the type and timing of sediment (siliciclastic or carbonate) supply as found to occur in other mixed carbonate–siliciclastic margin systems (Jorry et al., 2008). In reef-blocked canyons (e.g. Canyon 4; Figs. 2 and 6A), the sediment funnelled to the canyons will be almost exclusively carbonate and therefore depends on the nature of carbonate factory. In partly reef-blocked canyons, the sedimentary dynamics will be even more complicated due to the multiple sediment sources to a single canyon, and this behaviour may be different from one canyon to another. Future research on sediment cores and seismic reflection profiles will help to establish the precise sediment source in each canyon, composition and type SGF deposits, the onset of canyon activity, and to recognise periods of quiescence and/or stronger canyon activity.

5.3. Control of canyon morphology on depositional models: implications and further research

In the GBR, a transgressive shedding model of margin sedimentation is proposed to explain the shelf-to-basin sediment fluxes (Dunbar et al., 2000; Page et al., 2003; Francis et al., 2007). However, the possible role of submarine canyons in this model is not considered. The data and interpretations from this study have shown that the Ribbon Reef Canyons are important and active conduits for sediment delivery into the basin, and that large sediment accumulations on the seafloor are directly linked to submarine canyons. Therefore, these canyons could also condition the transgressive shedding depositional model in this part of the GBR, even though this model is based on mass accumulation rates of hemipelagic sediments and not explicitly on turbidite deposition. In the transgressive shedding model, the low flux of fine-grained, siliciclastic sediments to the Queensland Trough during sea-level lowstands is interpreted to be the result of the reef-ponding effect (i.e., sediments are trapped behind the reefs; Dunbar and Dickens, 2003b; Page et al., 2003). This interpretation seems to be inappropriate if the presence of submarine canyons is considered. Most of the Ribbon Reef Canyons' heads are indented in the shelf-break at less than 120 m water depth (Table 1, Figs. 2, 4 and 5), with some inter-reef passages characterised by excavated channels directly connected with canyon heads (Figs. 5A and 6C). In this scenario of well established shelf-basin connection via submarine canyons, it is difficult to envisage complete trapping of sediments behind the reefs over the entire system. Whether reefs acted as sediment traps during some positions of the sea-level curve, the inter-reef passages connected to canyons were likely to be the sole sediment pathways.

The complex morphology of the Ribbon Reef Canyon system has to be considered in the context of the transgressive shedding model as this morphology influences the pathways for the different sediment sources. In this study, we show that coarse-grained sediment supply to canyons has different sources (i.e. reef and/or shelf/channels). For example, in basin areas linked to canyons that are exclusively fed by

carbonate material (e.g. Canyon 4; Figs. 4A and 5), the transgressive shedding model might not be appropriate as coarse-grained siliciclastics would likely be very low or nil at all times.

To build on the general morphological characteristics and controls on the Ribbon Reef Canyons advanced in this study, further research must focus on characterising canyon systems along the entire GBR margin. First, these studies should focus on high-resolution multibeam mapping of the entire region to quantify the canyon distribution and morphology. Second, sub-bottom seismic profiles will help to characterise the canyon channel geometry and infilling deposits. Finally, these data, combined with detailed investigations of long sediment cores from the canyons, will provide the larger spatial and temporal framework needed to better assess what role the canyons play in delivering coarse-grained sediments to the basins.

6. Conclusions

Based on our detailed analysis of new high-resolution bathymetric and existing side-scan data, we draw the following conclusions:

1. The continental margin of the northern GBR along the Ribbon Reef region is excavated by submarine canyons that correspond to two main morphologically different canyons types: shelf-incised canyons (Type 1) and slope-confined canyons (Type 2).
2. The morphology of the extensive shelf-edge barrier reef (Ribbon Reefs) conditions the type of connection of the shelf-incised canyons resulting in: 1) reef-blocked canyons; 2) partly reef-blocked canyons; and 3) shelf-connected canyons. Shelf-incised canyons also influence the distribution of large SGF deposits on the basin floor.
3. The recent evolution of the submarine canyons has been influenced by the presence of the Ribbon Reefs. We argue that the degree to which the canyons heads are blocked by the reefs controls the sediment supply to the canyons and the type and frequency of eroding sediment gravity flows.
4. The Ribbon Reef Canyon system represents an active system. This activity is demonstrated by the presence of erosional features (e.g. submarine landslides) on the seabed, migrating submarine sandwaves and sediment gravity flows deposited on the canyons and basin floor which form small sediment lobes.

Supplementary materials related to this article can be found online at doi:10.1016/j.margeo.2011.09.013.

Acknowledgements

This research was supported by a James Cook University Faculty Grant Scheme, University of Sydney Start-Up funding, the Australian Marine National Facility for RV Southern Surveyor shiptime, National Geographic Society, and the Natural Environment Research Council. Ángel Puga-Bernabéu was additionally funded by a Postdoctoral Contract from the 'Plan Propio de Investigación' of the Universidad de Granada (Spain). R. Beaman acknowledges a Queensland Smart Futures Fellowship for salary support. V. Guilbaud performed his work during his MS thesis stay in Sydney and was supported by the Institut Universitaire Européen de la Mer at Brest (France). Constructive reviews by Peter Harris, two anonymous reviewers, and the editor, David J.W. Piper are greatly appreciated.

References

Abbey, E., Webster, J.M., Beaman, R.J., 2011. Geomorphology of submerged reefs on the shelf edge of the Great Barrier Reef: The influence of oscillating Pleistocene sea-levels. Marine Geology 288, 61–78. doi:10.1016/j.margeo.2011.08.006.

Alonso, B., Ercilla, G., 2003. Small turbidite systems in a complex tectonic setting (SW Mediterranean Sea): morphology and growth patterns. Marine and Petroleum Geology 19, 1225–1240.

Anderson, K.S., Graham, S.A., Hubbard, S.M., 2006. Facies, architecture, and origin of a reservoir-scale sand-rich succession within submarine canyon fill: insights from Wagon Caves Rock (Paleocene), Santa Lucia, California, U.S.A. Journal of Sedimentary Research 76, 819–838.

Antobreh, A.A., Krastel, S., 2006. Morphology, seismic characteristics and development of Cap Timiris Canyon, offshore Mauritania: a newly discovered canyon preserved off a major arid climatic region. Marine and Petroleum Geology 23, 37–59.

Arzola, R.G., Wynn, R.B., Lastras, G., Masson, D.G., Weaver, P.P.E., 2008. Sedimentary features and processes in the Nazaré and Setúbal submarine canyons, west Iberian margin. Marine Geology 250, 64–88.

Ashley, G.M., 1990. Classification of large-scale subaqueous bedforms: a new look at an old problem. Journal of Sedimentary Petrology 60, 160–172.

Babonneau, N., Sayoye, B., Cremer, M., Klein, B., 2002. Morphology and architecture of the present canyon and channel system of the Zaire deep-sea fan. Marine and Petroleum Geology 19, 445–467.

Bartholdy, J., Flemming, B.W., Bartholoma, A., Ernstsen, V.B., 2005. Flow and grain size control of depth-independent simple subaqueous dunes. Journal of Geophysical Research 110, F04S16.

Baztan, J., Berné, S., Olivet, J.L., Rabineau, M., Gaudin, D.M., Réhault, J.P., Canals, M., 2005. Axial incision: the key to understand submarine canyon evolution (in the western Gulf of Lion). Marine and Petroleum Geology 22, 805–826.

Beaman, R.J., 2010. 3DGBR. A high-resolution depth model for the Great Barrier Reef and Coral Sea. Marine and Tropical Sciences Research Facility (MTSRF) Project 2.5i.1a Final Report, MTSRF. 12 pp.

Beaman, R.J., Webster, J.M., Wust, R.A.J., 2008. New evidence for drowned shelf edge reefs in the Great Barrier Reef, Australia. Marine Geology 247, 17–34.

Beer, R.M., Gorsline, D.S., 1971. Distribution, composition and transport of suspended sediment in Redondo submarine canyon and vicinity (California). Marine Geology 10, 153–175.

Blakeway, D., 1991. Sedimentary sources and processes in outer shelf, slope and submarine environments, northern Ribbon Reefs, Great Barrier Reef, Australia. Unpublished BSc Honours Thesis, James Cook University, 143 pp.

Braithwaite, C.J.R., Montaggioni, L.F., 2009. The Great Barrier Reef: a 700 000 year diagenetic history. Sedimentology 56, 1591–1622.

Braga, J.C., Martín, J.M., Wood, J.L., 2001. Submarine lobes and feeder channels of redeposited, temperate carbonate and mixed siliciclastic-carbonate platform deposits (Vera Basin, Almería, southern Spain). Sedimentology 48, 99–116.

Carlson, P.R., Karl, H.A., 1988. Development of large submarine canyons in the Bering Sea, indicated by morphologic, seismic, and sedimentologic characteristics. Geological Society of America Bulletin 100, 1594–1615.

Carpenter, G., 1981. Coincident sediment slump/clathrate complexes on the U.S. Atlantic continental slope. Geo-Marine Letters 1, 29–32.

Chiang, C.S., Yu, H.S., 2006. Morphotectonics and incision of the Kaoping submarine canyon, SW Taiwan orogenic wedge. Geomorphology 80, 199–213.

Collier, J.S., Brown, C.J., 2005. Correlation of sidescan backscatter with grain size distribution of surficial seabed sediments. Marine Geology 214, 431–449.

Daly, R.A., 1936. Origin of submarine canyons. American Journal of Science 31, 401–420.

Davies, P.J., McKenzie, J.A., Palmer-Julson, A., et al., 1991. Proceedings of the Ocean Drilling Program Initial Reports 133. Ocean Drilling Program, College Station, TX.

Deptuck, M.E., Piper, D.J.W., Savoye, B., Gervais, A., 2008. Dimensions and architecture of late Pleistocene submarine lobes off the northern margin of East Corsica. Sedimentology 55, 869–898.

Dugan, B., Fleming, P.B., 2000. Overpressure and fluid flow in the New Jersey continental slope: implications for slope failure and cold seeps. Science 289, 288–291.

Dunbar, G.B., Dickens, G.R., 2003a. Late Quaternary shedding of shallow-marine carbonate along a tropical mixed siliciclastic-carbonate shelf: Great Barrier Reef, Australia. Sedimentology 50, 1061–1077.

Dunbar, G.B., Dickens, G.R., 2003b. Massive siliciclastic discharge to slopes of the Great Barrier Reef Platform during sea-level transgression: constraints from sediment cores between 15°S and 16°S latitude and possible explanations. Sedimentary Geology 162, 141–158.

Dunbar, G.B., Dickens, G.R., Carter, R.M., 2000. Sediment flux across the Great Barrier Reef Shelf to the Queensland Trough over the last 300 ky. Sedimentary Geology 133, 49–92.

Elliott, G.M., Shannon, P.M., Haughton, P.D.W., Praeg, D., O'Reilly, B., 2006. Mid- to Late Cenozoic canyon development on the eastern margin of the Rockall Trough, offshore Ireland. Marine Geology 229, 112–132.

Exon, N.F., Hill, P.J., Mitchell, C., Post, A., 2005. Nature and origin of the submarine Albany canyons off southwest Australia. Australian Journal of Earth Sciences 52, 101–115.

Farre, J.A., McGregor, B.A., Ryan, W.B.F., Robb, J.M., 1983. Breaching the shelfbreak passage from youthful to mature phase in submarine canyon evolution. SEPM Special Publication 33, 25–39.

Francis, J.M., Dunbar, G.B., Dickens, G.R., Sutherland, I.A., Droxler, A.W., 2007. Siliciclastic sediment across the North Queensland Margin (Australia): a Holocene perspective on reciprocal versus coeval deposition in tropical mixed siliciclastic-carbonate systems. Journal of Sedimentary Research 77, 572–586.

Francis, J.M., Daniell, J.J., Droxler, A.W., Dickens, G.R., Bentley, S.J., Peterson, L.C., Opdyke, B.N., Beaufort, L., 2008. Deep water geomorphology of the mixed siliciclastic-carbonate system, Gulf of Papua. Journal of Geophysical Research 113, F01S16.

Goodbred Jr., S.L., Kuehl, S.A., 2000. Enormous Ganges–Brahmaputra sediment discharge during strengthened early Holocene monsoon. Geology 28, 1083–1086.

Goff, J.A., Olson, H.C., Duncan, C.S., 2000. Correlation of side-scan backscatter intensity with grain-size distribution of shelf sediments, New Jersey margin. Geo-Marine Letters 20, 43–49.

Green, A., 2009. Sediment dynamics on the narrow, canyon-incised and current-swept shelf of the northern KwaZulu–Natal continental shelf, South Africa. Geo-Marine Letters 29, 210–219.
Green, A., Uken, R., 2008. Submarine landsliding and canyon evolution on the northern KwaZulu–Natal continental shelf, South Africa, SW Indian Ocean. Marine Geology 254, 152–170.
Green, A.N., Goff, J.A., Uken, R., 2007. Geomorphological evidence for upslope canyon-forming processes on the northern KwaZulu–Natal shelf, SW Indian Ocean, South Africa. Geo-Marine Letters 27, 399–409.
Harris, P.T., Whiteway, T., 2011. Global distribution of large submarine canyons: geomorphic differences between active and passive continental margins. Marine Geology 285, 69–85.
Heap, A.D., Harris, P.T., 2008. Geomorphology of the Australian margin and adjacent seafloor. Australian Journal of Earth Sciences 55, 555–585.
Herzer, R.H., Lewis, D.W., 1979. Growth and burial of a submarine canyon off Motunau, North Canterbury, New Zealand. Sedimentary Geology 24, 69–83.
Hopley, D., Smithers, S.G., Parnell, K.E., 2007. The Geomorphology of the Great Barrier Reef: Development, Diversity, and Change. Cambridge University Press. 546 pp.
Hughes Clarke, J.E., 1994. Toward remote seafloor classification using the angular response of acoustic backscattering: a case study from multiple overlapping GLORIA data. IEEE Journal of Oceanic Engineering 19, 364–374.
Hühnerbach, V., Masson, D.G., Bohrmann, G., Bull, J.M., Weinrebe, W., 2005. Deformation and submarine landsliding caused by seamount subduction beneath the Costa Rica continental margin—new insights from high-resolution sidescan sonar data. In: Hodgson, D.M., Flint, S.S. (Eds.), Submarine Slope Systems: Processes and Products: Geological Society, London, Special Publications, 244, pp. 195–205.
Inman, D.L., Nordstrom, C.E., Flick, R.E., 1976. Currents in submarine canyons: an air-sea-land interaction. Annual Review of Fluid Mechanics 8, 275–310.
Jorry, S.J., Droxler, A.W., Mallarino, G., Dickens, G.R., Bentley, S.J., Beaufort, L., Peterson, L.C., Opdyke, B.N., 2008. Bundled turbidite deposition in the central Pandora Trough (Gulf of Papua) since Last Glacial Maximum: linking sediment nature and accumulation to sea level fluctuations at millennial timescale. Journal of Geophysical Research 113, F01S19.
Karl, H.A., Cacchione, D.A., Carlson, P.R., 1986. Internal-wave currents as a mechanism to account for large sand waves in Navarinksy Canyon head, Bering Sea. Journal of Sedimentary Petrology 56, 706–714.
Kenyon, N.H., Klaucke, I., Millington, J., Ivanov, M.K., 2002. Sandy submarine canyon-mouth lobes on the western margin of Corsica and Sardinia, Mediterranean Sea. Marine Geology 184, 69–84.
Kineke, G.C., Woolfe, K.J., Kuehl, S.A., Milliman, J.D., Dellapenna, T.M., Purdon, R.G., 2000. Sediment export from the Sepik River, Papua New Guinea: evidence for a divergent sediment plume. Continental Shelf Research 20, 2239–2266.
Lastras, G., Arzola, R.G., Masson, D.G., Wynn, R.B., Huvenne, V.A.I., Hühnerbach, V., Canals, M., 2009. Geomorphology and sedimentary features in the Central Portuguese submarine canyons, Western Iberian margin. Geomorphology 103, 310–329.
Leach, A.S., Wallace, M.W., 2001. Cenozoic submarine canyon systems in cool water carbonates from the Otway Basin, Victoria, Australia. In: Hill, K.C., Bernecker, T. (Eds.), PESA-Eastern Australasian Basins Symposium, A Refocused Energy Perspective for the Future. PESA, Melbourne, Victoria, pp. 465–473.
Lewis, K.B., Barnes, P.M., 1999. Kaikoura Canyon, New Zealand: active conduit from near-shore sediment zones to trench-axis channel. Marine Geology 162, 39–69.
Ludman, D.M., 2007. Source, timing and frequency of turbidite deposits in the submarine canyons of the northern Great Barrier Reef. Unpublished BSc Thesis, James Cook University, Australia, 103 pp.
Maxwell, W.G.H., 1968. Atlas of the Great Barrier Reef. Elsevier, Amsterdam. 258 pp.
Maxwell, W.G.H., Swinchatt, J.P., 1970. Great Barrier Reef: regional variation in a terrigenous-carbonate province. Geological Society of America Bulletin 81, 691–724.
McAdoo, B.G., Pratson, L.F., Orange, D.L., 2000. Submarine landslide geomorphology, US continental slope. Marine Geology 169, 103–136.
Mitchell, J.K., Holdgate, G.R., Wallace, M.W., Gallagher, S.J., 2007. Marine geology of the Quaternary Bass Canyon system, southeast Australia: a cool-water carbonate system. Marine Geology 237, 71–96.
Mountjoy, J.J., Barnes, P.M., Pettinga, J.R., 2009. Morphostructure and evolution of submarine canyons across an active margin: Cook Strait sector of the Hikurangi Margin, New Zealand. Marine Geology 260, 45–68.
Mulder, T., Alexander, J., 2001. The physical character of subaqueous sedimentary density flows and their deposits. Sedimentology 48, 269–299.
Mulder, T., Syvitski, J.P.M., Migeon, Sébastien, Faugéres, J.C., Savoyed, B., 2003. Marine hyperpycnal flows: initiation, behaviour and related deposits. A review. Marine and Petroleum Geology 20, 861–882.
Mullenbach, B.L., Nittrouer, C.A., Puig, P., Orange, D.L., 2004. Sediment deposition in a modern submarine canyon: Eel Canyon, northern California. Marine Geology 211, 101–119.
Nanson, G.C., Price, D.M., Short, S.A., Young, R.W., Jones, B.G., 1991. Comparative uranium-thorium and thermoluminescence dating of weathered Quaternary alluvium in the tropics of northern Australia. Quaternary Research 35, 347–366.
Nott, J., Price, 1994. Plunge pools and paleoprecipitation. Geology 22, 1047–1050.
Orange, D., Breen, N., 1992. The effects of fluid escape on accretionary wedges 2. Seepage force, slope failure, headless submarine canyons, and vents. Journal of Geophysical Research Oceans 97, 9277–9295.
Orange, D.L., McAdoo, B., Moore, C.J., Tobin, H., Screaton, E., Chezar, H., Lee, H., Reid, M., Vail, R., 1997. Headless submarine canyons and fluid flow on the toe of the Cascadia accretionary complex. Basin Research 9, 303–312.
Page, M.C., Dickens, G.R., Dunbar, G.B., 2003. Tropical view of Quaternary sequence stratigraphy: siliciclastic accumulation on slopes east of the Great Barrier Reef since the Last Glacial Maximum. Geology 31, 1013–1016.
Piper, D.J.W., Hiscott, R.N., Normark, W.R., 1999. Outcrop scale acoustic facies analysis and latest Quaternary development of Hueneme and Dume fans, offshore California. Sedimentology 46, 47–78.
Popescu, I., Lericolais, G., Panin, N., Normand, A., Dinu, C. Le, Drezen, E., 2004. The Danube submarine canyon (Black Sea): morphology and sedimentary processes. Marine Geology 206, 249–265.
Posamentier, H.W., Vail, P.R., 1988. Eustatic control on clastic deposition II—sequence and system tracts models. In: Wilgus, C.K., Hastings, B.S., Posamentier, H., Van Wagoner, J., Ross, C.A., Kendall, C.G.St.C. (Eds.), Sea Level Changes: An Integrated Approach: SEPM Special Publication, 42, pp. 125–154.
Pratson, L.F., Coakley, B.J., 1996. A model for the headward erosion of submarine canyons induced by downslope-eroding sediment flows. Geological Society of America Bulletin 108, 225–234.
Pratson, L.F., Ryan, W.B.F., Mountain, G.S., Twichell, D.C., 1994. Submarine-canyon initiation by downslope-eroding sediment flows: evidence in late Cenozoic strata on the New-Jersey continental-slope. Geological Society of America Bulletin 106, 395–412.
Puga-Bernabéu, Á., Martín, J.M., Braga, J.C., 2008. Sedimentary processes in a submarine canyon excavated into a temperate-carbonate ramp (Granada Basin, southern Spain). Sedimentology 55, 1449–1466.
Puig, P., Ogston, A.S., Mullenbach, B.L., Nittrouer, C.A., Sternberg, R.W., 2003. Shelf-to-canyon sediment-transport processes on the Eel continental margin (northern California). Marine Geology 193, 129–149.
Ridente, D., Foglini, F., Minisini, F.T., Verdicchio, G., 2007. Shelf-edge erosion, sediment failure and inception of Bari Canyon on the Southwestern Adriatic Margin (Central Mediterranean). Marine Geology 246, 193–207.
Ruiz-Ortiz, P.A., de Gea, G.A., Castro, J.M., 2006. Timing of canyon-fed turbidite deposition in a rifted basin: the Early Cretaceous turbidite complex of the Cerrajón Formation (Subbetic, Southern Spain). Sedimentary Geology 192, 141–166.
Shanmugam, G., 2003. Deep-marine tidal bottom currents and their reworked sands in modern and ancient submarine canyons. Marine and Petroleum Geology 20, 471–491.
Shanmugam, G., Shrivastava, S.K., Das, B., 2009. Sandy debrites and tidalites of Pliocene reservoir sands in upper-slope canyon environments, offshore Krishna–Godavari Basin (India): implications. Journal of Sedimentary Research 79, 736–756.
Shepard, F.P., 1972. Submarine canyons. Earth-Science Reviews 8, 1–12.
Shepard, F.P., Dill, R.F., 1966. Submarine Canyons and Other Sea Valleys. Rand McNally, Chicago, Illinois. 381 pp.
Shepard, F.P., Marshall, N.F., McLoughlin, P.A., 1974. Currents in submarine canyons. Deep Sea Research 21, 691–706.
Smith, D.P., Ruiz, G., Kvitek, R., Iampietro, P.J., 2005. Semiannual patterns of erosion and deposition in upper Monterey Canyon from serial multibeam bathymetry. Geological Society of America Bulletin 117, 1123–1133.
Smith, D.P., Kvitek, R., Iampietro, P.J., Wong, K., 2007. Twenty-nine months of geomorphic change in upper Monterey Canyon (2002–2005). Marine Geology 236, 79–94.
Soh, W., Tokuyama, H., 2002. Rejuvenation of submarine canyon associated with ridge subduction, Tenryu Canyon, off Tokai, central Japan. Marine Geology 187, 203–220.
Symonds, P.A., Davies, P.J., Parisi, A., 1983. Structure and stratigraphy of the Central Great Barrier Reef. Bureau of Mineral Resources Journal of Australian Geology and Geophysics 8, 277–291.
Twichell, D.C., Roberts, D.G., 1982. Morphology, distribution, and development of submarine canyons on the United States Atlantic continental slope between Hudson and Baltimore Canyons. Geology 10, 408–212.
Webster, J.M., Davies, P.J., 2003. Coral variation in two deep drill cores: significance for the Pleistocene development of the Great Barrier Reef Sedimentary. Geology 159, 61–80.
Webster, J.M., Beaman, R.J., Bridge, T.C.L., Davies, P.J., Byrne, M., Williams, S., Manning, P., Pizarro, O., Thornborough, K., Woolsey, E., Thomas, A.L., Tudhope, A., 2008a. From corals to canyons: the Great Barrier reef margin. EOS, Transactions, American Geophysical Union 89, 217–218.
Webster, J.M., Davies, P.J., Beaman, R.J., Williams, S., Byrne, M., 2008b. Evolution of drowned shelf edge reefs in the GBR; implications for understanding abrupt climate change, coral reef response and modern deep water benthic habitats. RV Southern Survey — voyage summary. Marine National Facility, p. 18. http://www.marine.csiro.au/nationalfacility/voyagedocs/2007/summarySS07-2007.pdf.
Webster, J.M., Ludman, D., Wust, R., Beaman, R., Renema, W., Moss, P., 2008c. Sediment Flux and Composition Changes in Canyons Along a Mixed Carbonate–Siliciclastic Margin: Evidence From Turbidite Deposits Along the Great Barrier Reef Margin. American Association of Petroleum Geologists, San Antonio, Texas, United States.
Webster, J.M., Yokoyama, Y., Cotterill, C., and the Expedition 325 Scientists, 2011. Proceedings of the Integrated Ocean Drilling Program, 325. Tokyo. Integrated Ocean Drilling Program Management International, Inc.
Wynn, R.B., Stow, D.A.V., 2002. Classification and characterisation of deep-water sediment waves. Marine Geology 192, 7–22.
Wynn, R.B., Douglas, G.M., Bett, B.J., 2002. Hydrodynamic significance of variable ripple morphology across deep-water barchans dunes in the Faroe–Shetland Channel. Marine Geology 192, 309–319.
Xu, J.P., Wong, F.L., Kvitek, R., Smith, D.P., Paull, C.K., 2008. Sandwave migration in Monterey Submarine Canyon, Central California. Marine Geology 248, 193–212.